Introduction to 3D design problem

By Kees Hornman (Shell Gabon) and Gijs Vermeer (3DSymSam - Geophysical Advice)

Introduction

For the workshop '3D Seismic surveys: design, tests and experience' held at the 61st EAGE Conference on June 5th 1999, five specialists in the design of 3D surveys were invited to recommend survey design parameters, based on a common case study. Participants were Mike Galbraith (Seismic Image Software), Malcolm Lansley (Western Geophysical), Julien Meunier (CGG), David Monk (Continuum Resources) and Jim Musser (Green Mountain Geophysics). Their recommendations are reproduced in the articles following this introductory paper.

Case study

A 3D survey of some 380 full-fold km^2 is to be acquired in a land area, reasonably densely populated, with cultivated dunes 30 m high by 500 m across. The N-S extent of the survey is some 40 km, the E-W extent is on average 9.2 km. Although the geophysical requirements are the primary driver of the 3D design, the parameters should be realistic and for that reason some very simple cost escalation factors have been given to the specialists.

Previous work in the area

A 2D Vibroseis survey was acquired in the area with a spacing of approximately 5 km between the lines. Most of these lines were acquired with a shotpoint and group interval of 25 m, but a few test lines were acquired with 20 m intervals; all lines had a multiplicity of 180. The specialists have access to two intersecting lines, one with an interval of 20 m ('line A'), the other with an interval of 25 m ('line B'). At the intersection of the two lines, another experiment was carried out: the complete spread was laid out as 6 connected parallel lines, 600 m apart, length about 5000 m, and the vibrators zig-zagged between the stationary receiver lines, to create a mini-3D with varying fold. The figure shows the time map in ms (blue = 2100, orange = 2200 ms), and the reflection amplitudes for this mini 3D. Finally, it should be mentioned that a typical stacking velocity profile shows velocities increasing from 1750 m/s near the surface to 2300 m/s at 1s, 2500 m/s at 2 s. The ground-roll velocity varies, 250-350 m/s are commonly observed values.

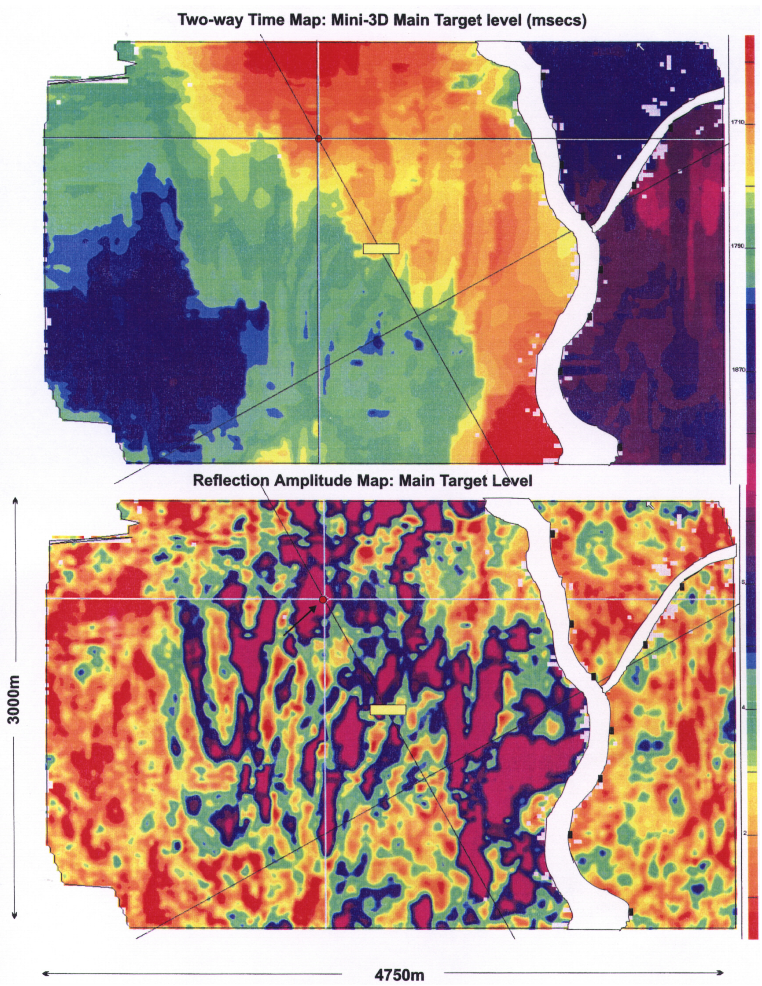

Description of geology and challenges

A lignite layer overlies the three targets, the main target at some 2000 m depth, the other two at depths of 2500 and 3000 m. All three targets may feature dips up to 20°. Trapping in the main target may be stratigraphic in addition to structural. The main challenges are to resolve the stratigraphic complexity at the main target and the interpreter requires a vertical resolution of about 14 m, a horizontal resolution of 50 m. The velocity inversion at the lignite causes multiples and transmission losses, the presence of dunes causes statics problems.

Cost escalation factors

Although the survey design is based on a real prospect, no actual cost estimates exist for different designs. We have provided the designers with an artificial cost factor formula primarily to prevent extreme solutions, such as a design with 10 000 channels. In order to keep the problem simple we have selected a few parameters only, which we consider to be the most important contributors to the cost of the survey, based on experience with 2D data:

1. Number of active cables C
2. Cable density D (in km of cable per square km surface)
3. Geophones per array G
4. Group interval R (in m)
5. Number of active channels N
6. Shotline density S (in km per square km)
7. Shotpoint spacing V (in m)

The final cost factor is estimated by:
*Costs =(0.94+0.01*C)*(D/2.5)*(0.033*G+0.2)*(5/R+0.9)*(2880/(3600-N))*(S/2.5)*(13.5/V+0.73)*
It will be seen that the case of C = 6, D = 2.5, G = 24, R = 50, N = 720, S = 2.5 and V = 50 will lead to a relative cost of 1.

3D Seismic Survey Design: a solution by

Mike Galbraith, *Seismic Image Software Ltd.*

Introduction: In this short paper, we define the 3D-design problem (more fully stated elsewhere), establish the basic 3D parameters (bin size, maximum offset, shot/receiver line spacings, patch size, fold). We then propose some geometries for this area and analyse the performance of each from a geophysical viewpoint (e.g. are they artefact free?). Finally we make our recommendations.

Objectives:

The basic objectives and problems are:

Three separate targets at 2000 m, 2500 m and 3000 m - all with dips up to 20^o,

Shallow (Main) target is stratigraphic and structural requiring 14 m vertical resolution and 50 m horizontal.

Lignite at 1250 m causes multiples and transmission losses,

Ground roll is present on 2D data (velocities from 500 m/s to 300 m/s),

Statics are related to dunes and can be severe,

Obstacles not severe,

Vibroseis is preferred source.

Basic Parameters: To establish the basic 3D parameters, two 2D models were built along Line A and along Line B. The model for Line A is shown in Figure 1.

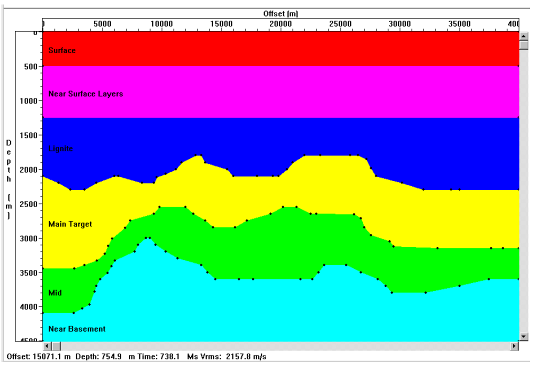

Figure 1. Model for Line A

Using the models and existing information, the basic parameters were established as follows:

Bin Size: From amplitude spectra of the 2D data and examining the mini-3D, the maximum useful frequency is approximately 70 Hz at the main target – and diminishing with depth. In addition, the dominant (or average) signal frequency could be as high as 50 Hz.

Using the standard anti-aliasing formula:

Bin size = $V_{interval}/(4f_{max}\sin\theta)$;

we can see that required bin sizes for dips of 20^o are as follows:

Main Target	26 m ($V_{interval}$ = 2500 m/s)
Mid Target	42 m ($V_{interval}$ = 4000 m/s)
Near Basement	52 m ($V_{interval}$ = 5000 m/s)

Using resolution formulae (Vermeer, 1999) we calculate the maximum frequency for 14 m vertical resolution, assuming depth equals offset.

$f_{max} = (c/2).(v/(R_z.\cos i))$, gives f_{max} = 71 Hz (c = 0.715, v = 2500 m/s , R_z = 14m, cosi = 0.9).

Horizontal resolution, R_x is affected by migration aperture. Using Vermeer (1999), we have:

$R_x = cv/(2.f_{max}.\sin\theta\cos i)$ = 28 m, assuming f_{max} = 71 Hz, θ = 30^o (this is the migration aperture normally used in design), cosi = 0.9.

Thus, if we can achieve a maximum signal frequency of 71 Hz at our target the desired vertical (14 m) and horizontal (50 m) resolution can be achieved.

An analysis of the 2D stack trace amplitude spectra, using 400 ms windows above and below 1.0 s (approximately the time of the Lignite layer) reveals that frequencies from 0 – 60 Hz have similar amplitudes in both windows and a relatively sharp drop in amplitudes above 60 Hz for the window below 1 sec. compared to the window above. The amplitude at 70 Hz is approximately 5 dB below 60 Hz for the shallow window and is 10 dB below 60 Hz for the deep window. This indicates that 71 Hz can be achieved, albeit weakly, at the target time of 2 s. Some consideration might be given to ways to improve the 70 Hz energy at 2 s (longer sweeps, more ground force, non-linear sweep, etc.).

The required bin size is related to the signal sampling interval required to avoid aliasing. Margrave (1997) advocates the use of the interval velocity at the target. In this case the velocity used in the formula above (2500 m/s) represents an average of several layers above the target. The interval velocity can be chosen as small as 2100 m/s (the Lignite layer velocity immediately above the Main Target), leading to a bin size of 21 m. The minimum required bin size is therefore 21 m and may be relaxed to 26 m. using a velocity of 2500 m/s (standard anti-aliasing formula above). Thus reasonable choices might be 20, 25 or 30 m. Smaller bins imply higher cost. Larger bins imply less resolution. If other 3D's were available for comparison purposes, a choice of 30 m might be made. Note that using a bin size = 25m with velocity = 2100 m/s can be justified if f_{max} is smaller than 71 Hz (need 61 Hz), or if we have a smaller dip angle at depth (θ=17.5^o), or higher velocity (2500 m/s). Dip angle and velocity are difficult to change. Smaller maximum frequency means desired resolution will suffer. In this case 20 m is a safe choice but economics suggests 25 m. For this paper, therefore, we shall use a bin size = 25 m. Shot and receiver spacing is $\Delta s = \Delta r$ = 50 m.

Largest Minimum Offset and line spacing: There are no requirements for a shallow horizon (first desired one is at 2000 m), thus line spacing will be dictated by a need to achieve fold rather than a need to image a shallow horizon. Wide line spacing means a greater diversity of near trace offsets. Thus some bins (along the shot and receiver lines) will have many near traces while other bins will only have near traces with offsets equal to the largest minimum offset. This has possible consequences (i.e. stronger artefacts) for noise (linear and multiple) attenuation.

Maximum Offset: Using software and the models, the NMO stretch mute function was calculated – and compared to the actual mute used on the 2D.
The mute function in Figure 2 shows the maximum useful offsets corresponding to the various targets. We may summarise this as:

Main Target: X_{max} = 2150 m
Mid: X_{max} = 2550 m
Near Base. X_{max} = 4000 m

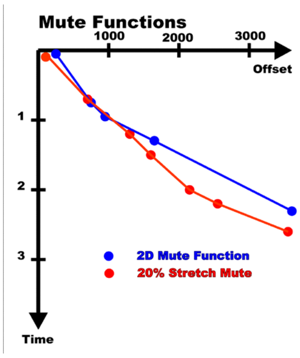

Figure 2 Comparison of mute functions

Patch Size: Assuming a maximum useful offset of 4000 m, we show two choices of SLI (shot line interval) and RLI (receiver line interval) and consequential fold, assuming one full shot salvo per (square) patch:

SLI = RLI = 200: NC = 6400: Fold = 400
SLI = RLI = 400: NC = 3200: Fold = 100

Clearly, if we wish higher fold with fewer channels (increase receiver line interval), we must increase the number of shots (by making the shot line interval less). The channel count is a consequence of the need to place receivers every 50 m and to have 4000 m offsets all within a square patch. Thus smaller receiver line intervals increase the channel count. The mini-3D achieved high fold through the use of double zigzag geometry, and we now investigate this. First, we calculate and display the average fold for each target in the mini-3D:

Main Target: 50
Mid: 67
Near Base. 144

Fold: Below we show fold calculations made from:

"Fold = π.offset^2/(4.SLI.RLI)"

for different line intervals (SLI=RLI) at each of the 3 targets. Note that the use of a double zigzag will double all fold values (twice the number of shots).

Line Interval	Nchannel	Fold Main	Fold Mid	Fold Deep
200	6400	91	128	314
300	4267	40	57	140
400	3200	23	32	79
500	2560	15	20	50
600	2133	10	14	35

Thus a 600 m line interval does not achieve good fold on any of the targets (10, 14 and 35). The number of channels is calculated for the total patch (8000 m square).
2D data had 180 fold and reasonable S/N. The mini-3D also appears to have good S/N. Ground roll is strong on supplied 2D shot data. The stratigraphic requirement means high fold to determine target amplitudes more exactly. And multiples from the Lignite are also very strong – again implying high fold for good attenuation. We will therefore aim to match or exceed the fold of the mini-3D at each target level.

Proposed Designs
Based on the recommendations above (bin size = 25 m, X_{max} = 4000 m, matching or exceeding mini-3D fold, square patch for better response to obstruction necessitated moves, statics coupling, imaging, multiple and linear noise attenuation – McGinn, 1998), we propose the following 6 alternatives:

A: SI = RI = 50, SLI = RLI = 300
Patch = 160 x 20, Geometry = Orthogonal
Fold at X_{Main} = 40, X_{Mid} = 56 X_{bot}= 116

B: SI = RI =50, SLI = RLI = 300
Patch = 160 x 20, Geometry = Single Zigzag
Fold at X_{Main} = 40, X_{Mid} = 56 X_{bot} = 116

C: SI = RI = 50, SLI = RLI = 400
Patch = 160 x 20, Geometry = Double Zigzag
Fold at X_{Main} = 45, X_{Mid} = 64 X_{bot} = 157

D: Same as C, but symmetrical shot lines.

E: SI = RI = 50, SLI = RLI = 200
Patch = 144 x 6, Geometry = Double Zigzag
Fold at X_{Main} = 64, X_{Mid} = 75 X_{bot} = 108

F: SI = RI = 50, SLI = RLI = 200
Patch = 144 x 12, Geometry = Double Zigzag
Fold at X_{Main} = 120, X_{Mid} = 150 X_{bot} = 216

Note that geometries E and F do not use square patches because of the very high fold built up by the extra shots and small RLI. Thus receiver lines were removed to reduce fold.
In each case, receiver lines are oriented EW (along Line B direction). Logistically, sweeping can proceed EW between receiver lines. At the end of each shot line (or double shot line), one receiver line will become free and can be re-laid further south (or north depending on preferred direction of travel). If enough equipment is available it will be possible to lay receiver lines across

the entire EW width of the survey.

X_{max} can be shortened with no change to the 6 geometries. The only effect will be fewer receivers per line: e.g. 4000 m requires 160, 3600 m requires 144 – and therefore 2880 channels rather than 3200. Our targets will also be unaffected (except for the deepest, which will lose some fold). So if equipment shortage is a problem a smaller patch can be used. The width (20 lines or 8000 m) can also be shortened. E.g. 12 or 14 lines is adequate to resolve the main and mid targets using a square patch. This reduces our channel count to 14 x 144 or 2016. Geometry E is a narrow patch (Xinline = 3600 m, Xcrossline = 600 m) – so cross-line imaging must be checked. Number of channels required is only 864, but many more shots make up the required fold.

As a practical note, the choice of recorder will affect the number of channels per receiver line – to fully utilise an exact number of "boxes". (e.g. Fairfield Box – multiple of 8, I/O II, multiple of 6, and so on for SN388, ARAM, etc.)

In all our designs the source will be Vibroseis. The following formula (Lansley, 1992):

S/N improvement in dB = 20 log (number of vibrators * fundamental ground force * (sweep length * number of sweeps * bandwidth of sweep) $^{1/2}$)

should be kept in mind when testing parameters such as sweep length, etc. In addition, new techniques such as Slip-Sweep (Wams, 1998) and HFVS (Allen, 1998) can dramatically affect production rates and therefore costs.

Analysis of Designs

The 6 designs A, B, C, D, E, F were subjected to the following systematic analyses (shown in Figures 3, 4 and 5):

(1) Calculation and display of fold at each target as verification of theoretical fold.

(2) Display of Offset Mix in all bins of a "unit cell" (area of bins between 2 shot and 2 receiver lines) in the centre of the survey (Figure 3). Each of the 6 graphs shows the offsets (vertical axis – offset increases upwards) for each CMP bin (horizontal axis). A and B exhibit "holes" at mid and far offsets and very sparse near traces. C shows strong repetitions and a sparse near trace mix. D is similar to A and B. E and more so F has no "holes" and a good mix of near traces.

(3) Display of Surface fold to check surface consistency. All geometries were adequate in this regard and good statics solutions would result. Statics coupling is almost always ensured by the many small shot and receiver position changes which occur in most 3D's

(4) Calculation of velocity "resolution" at Main Target. All geometries show that a conventional velocity analysis could determine velocity with an accuracy of +- 40 m/s

(5) Calculation of the Multiple response in all bins of a "unit cell".(Figure 4) The model used was a (flat) multiple of velocity 2250 m/s (Lignite event at 1.0 s) placed at a time of 2.0 sec. and NMO corrected with a velocity of 2500 m/s. In each bin, the offsets were NMO'd and CMP stacked. A search of the maximum amplitude was done and displayed as a colour value in the bin. The relative differences from one bin to its neighbours indicate the extent of an artefact due to multiples. The algorithm used here did not mute the near traces – a common practice when strong multiples are present. Thus the absolute values of the amplitudes observed are higher for those geometries which have more near traces (e.g. F). A and E have no strong pattern. B and D have a noticeable pattern. C has a significant pattern where the multiple remnants would definitely obscure the data. F has the smallest pattern in terms of the ratio of minimum and maximum amplitudes.

(6) Calculation of Linear Noise response in all bins of a "unit cell" (Figure 5). The model used was a linear velocity train (300 m/s) present on all traces at increasing time vs. offset. The traces were NMO corrected with a velocity of 2500 m/s and CMP stacked. A search of the maximum amplitude was done in a window of length 200 ms centred at 2.0 s and displayed as a colour value in the bin. Again, differences from one bin to the next indicate the extent of a noise (geometry) artefact. A has some pattern while B, C and D have very strong patterns of noise remnants. Both E and F show very small bin to bin variations.

(7) DMO response wavelets in "unit cell" for dip of 20^{o} at main target level –oriented NS (Line A). (Figure 6) This is potentially the worst case for DMO when the receiver lines are oriented EW (i.e. cross-line sampling vs. in-line sampling). Some pattern is evident in A, B and D. C is very strong. E and F have a negligible pattern.

Stack Response: Finally the 2D data was used to construct a 3D volume with offsets given by the various geometries. Thus the data was completely flat. Geometries B and F were evaluated by applying NMO and stack. Figure 7 shows the stack of geometry B.

Two events at times 996 ms and 1830 ms were examined for amplitude variations (Figure 8). Geometry B shows 2:1 variations in amplitude on the shallow event (996 ms) and 50% variations on the deep event (1830 ms). The 2D data used for this analysis was created by doing a common offset stack of 12 shots. Thus it contained both linear shot noise and multiple energy, though in lesser amounts than on the original shots. The process of NMO and stack did not entirely remove this energy. Such noise remnants would cause severe problems – even after migration. F shows 30% variations on the shallow event and less than 10% variations on the deep event. Such amplitude effects can be almost completely attenuated by migration.

Recommendations

Geometries E and F had the best performance for noise attenuation. Orthogonal geometries (A, for example) with square patches are known as good candidates for imaging. In this case, however, significant noise remnant patterns will lead to disruption of the final migrated image. Therefore the choice here favours geometries which best attenuate the various forms of noise.

References

Allen K.P. et al, 1998, High Fidelity vibratory Seismic (HFVS) Method for Acquiring Seismic Data: SEG Convention Abstracts, New Orleans, 1998.

Lansley, R.M., 1992, Reducing the cost of land 3D surveys: Vibroseis workshop, EAGE Convention, 1992.

Margrave, G.F., 1997, Seismic acquisition parameter considerations for a linear velocity medium, CSEG 1997.

McGinn, A. et al, 1998, Land Seismic data quality improvements: Leading Edge, Nov 1998.

Vermeer, G.J.O., 1999, Guidelines for Land 3D Geometry Design: SIS Seminar, Calgary, Mar.99.

Wams J., et al 1998, Recent developments in 3-D acquisition techniques using Vibroseis in Oman: Leading Edge, Aug 1998.

Figure 3 –Offset Mix in Geometries A to F. Note lack of near offsets in many bins and periodic "holes" at all offsets. Colour indicates many duplicate offsets.

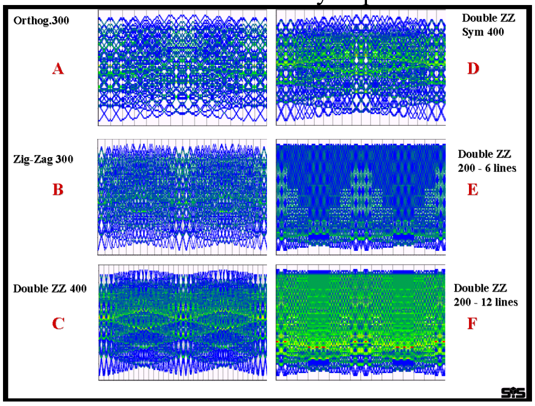

Figure 4 –Multiple Attenuation in Geometries A to F

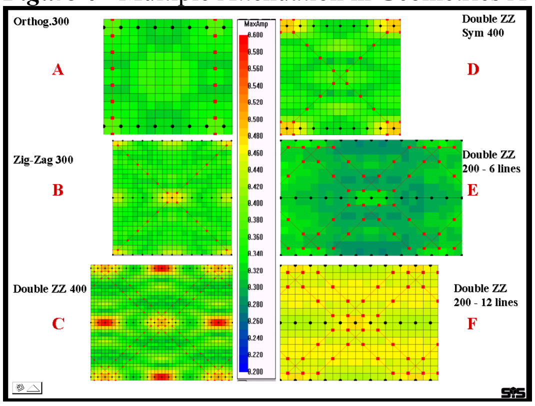

Figure 5–Linear Noise Attenuation in Geometries A to F

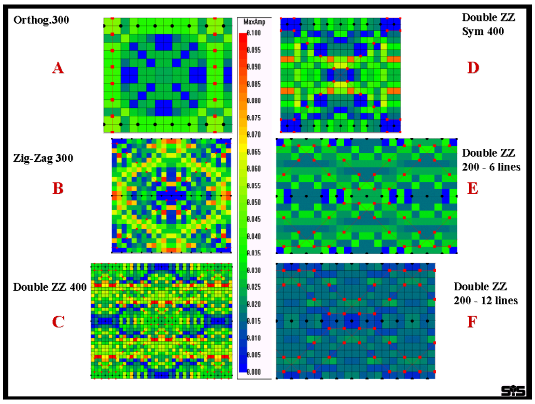

Figure 6 –DMO Response in Geometries A to F

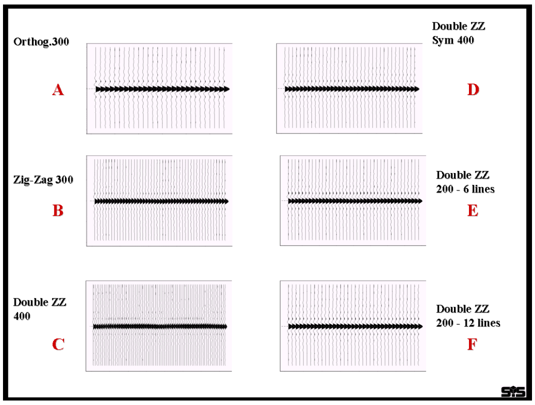

Figure 7 –Stack Response of B – note strong noise remnant patterns.

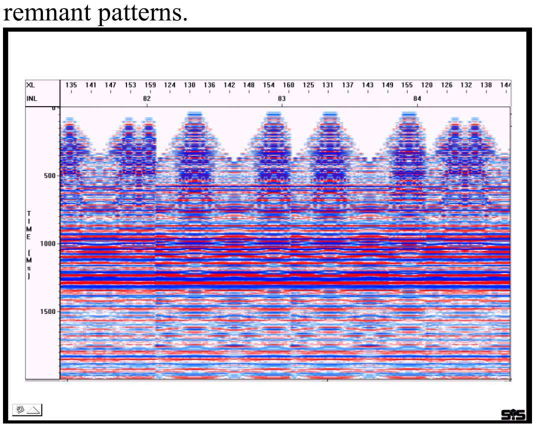

Figure 8 –Stack Response of B and F – time slices

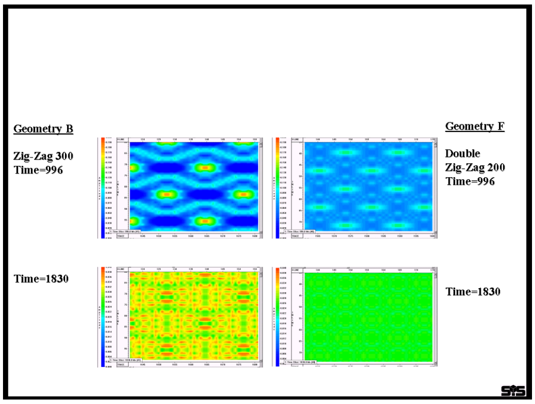

3D Seismic Survey Design: a solution by

Malcolm Lansley, *Western Geophysical*

Introduction

Analysis of the various geophysical challenges presented by the workshop organisers shows a considerable range in the relative levels of difficulty presented. It was felt that because of the inter-relationship between the different problems the best way in which to accomplish the design objectives can be summarised as follows. Acquire a survey with a very high trace density, with fine spatial sampling, and using small arrays. The difficulty lies in achieving this in a cost-effective manner.

Discussion

The first of the challenges, which is that of having three targets at different depths, is one of the less difficult problems to solve. This challenge is routinely met in many survey design projects and since the shallowest target is at approximately 2400 m, as long as the survey has a high trace density it should still be possible to acquire a good offset distribution in order to get adequate multiple attenuation.

In order to achieve vertical resolution of 14 m, it is necessary to design the survey in a manner that is consistent with the preservation of broadband signals at all stages of the acquisition and processing. Merely providing a broadband source will not solve this issue. There have been a number of different equations for vertical resolution; the two most commonly used being the Rayleigh criterion and another by Widess (1982). Since Rayleigh's equation is the more stringent in terms of high frequency requirements, I decided to use it, as I did not want to under-design the survey. Rayleigh's equation states that the resolution limit is at one-quarter wavelength of the dominant frequency.

$$\textit{Vertical resolution} \approx \frac{V_{\mathrm{int}}}{4 f_{dom}}$$

This means that for an interval velocity of 3700 m/s at the deepest target level, a dominant frequency of between 65 and 70 Hz must be retained. In order to obtain a 70 Hz dominant frequency, it will be necessary to record the data with a vibrator sweep that exceeds 110 Hz at the high frequency. Use of a non-linear sweep would probably help in achieving this, and should be evaluated in the field during the crew's initial startup tests.

For the horizontal resolution requirements of 50 m, small spatial sampling is obviously necessary. Again, there are several equations relating horizontal resolution (Denham and Sheriff (1980), Claerbout (1985), Embree (1985), Ebrom et al (1995), Vermeer (1996)) to the primary attributes of the data (interval velocity and dominant frequency) but all of these ignore the most critical factor, which is the velocity field used in the migration. A 0.5% error in the migration velocity can degrade the horizontal resolution by a factor of more than 5 (Deregowski et al, 1997). Figure 1 shows the residual Fresnel zones after migration with incorrect velocities, compared with the theoretical horizontal resolution. Once more, this implies that a high trace density with good offset sampling will be beneficial. Not only will this provide for better resolution in the actual migration process, but will also provide the data necessary to get very good velocity control.

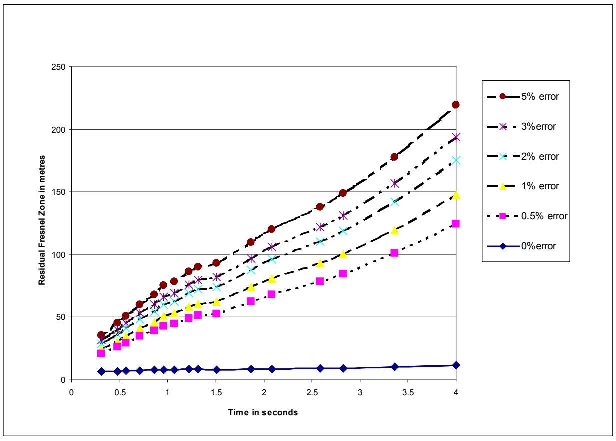

Figure 1 *Residual Fresnel zones for* a *dominant frequency of 70 Hz after migration with incorrect velocities (from 0.5% error to 5%) compared with the theoretical resolution (0% error).*

The dune-related static corrections are seen as less of a problem for the determination of the near-surface model, but as a much more significant problem for the preservation of high frequency signals. Analysis of the elevations and the resultant static corrections shows that the average velocity through the sand dunes is approximately 600 m/s. With such a low velocity layer, any significant variation in the elevation of different elements of the source and receiver arrays will lead to attenuation of the high frequencies (Embree 1978 and 1985).

It is therefore suggested that the physical dimension of both source and receiver arrays be minimised. The original surveys had been acquired using four vibrators. In order to preserve 110 Hz with no more than 3 dB of attenuation the total elevation difference between the first and last vibrator within the source array would need to be less than two m. If we use two vibrators, the length of the source array will be lessened and the maximum elevation difference permissible across the array will be reduced to less than one and a half metres. It is understood that the total sweep time (the product of the number of sweeps and the sweep length) may have to be increased with the use of two vibrators instead of four (Lansley, 1992). However, the signal to random noise ratio on the shot records provided appears to be quite good, and it may not be necessary to increase the sweep time by a factor of four, as Lansley's equations would suggest. The required sweep effort should be evaluated in the field during the crew's initial startup tests. The use of two (or more) sets of two vibrators will make movement through the farming communities easier, and the reduced output may also help in community relations and possibly lower the number of damage claims.

For the receiver arrays, the original 2-D surveys had used 12 geophones per group, and in the cost equation the unit cost standard 3-D survey has 24 geophones per group. It is recommended that the size of the geophone array also be decreased to reduce the amount of high frequency attenuation. A reduction to either six or three geophones per group will achieve this, as well as reducing the cost of the data acquisition. Coherent noise wavelengths are too long to be significantly attenuated by the geophone arrays without also attenuating the required higher signal frequencies. Random noise should be well attenuated in the imaging processes because of the high trace density. Krohn et al (1991) showed significant attenuation of high frequencies in the very near surface and the benefits of burying the geophones when high frequencies are required. This should be evaluated during field testing.

For the steep dips at depth, and in order to preserve the required high frequencies through the imaging processes, fine spatial sampling is recommended. By considering curved raypaths it would be possible to argue that a larger bin size would allow adequate spatial sampling to avoid spatial aliasing in the imaging processes. Even though a bin may be small enough to avoid migration aliasing, if conventional DMO (not “fat” or “wide”) and CMP stack are going to be applied to the data there can be unavoidable attenuation of high frequencies in the stacking process because of the dip across the bin. A bin size of 12.5 x 12.5 m will provide adequate sampling to preserve 110 Hz without aliasing and without significant frequency attenuation because of the dip across the bin.

In order to determine the required trace density (and hence the fold) the equation published by Krey (1987) for estimating 3D fold based on previously acquired 2D data can be used. If it is assumed that the signal to noise ratio of the 2D data is adequate, the trace density for each of the target depths can be calculated from the 2D fold for the required frequencies. An offset equals depth mute was assumed as this approximates quite well the first break suppression mute which had been applied in stacking. Since there is a range of target depths, and there were two different 2D lines provided which had different CMP intervals, a range of trace densities was determined for each target formation using the appropriate depths, velocities and CMP intervals:

shallow target	185 000 - 289 000 traces/km^2
middle target	256 000 - 400 000 traces/km^2
deep target	306 000 - 430 000 traces/km^2

These trace densities may appear to be quite high, but Krey’s equation shows that the required trace density is linearly related to the frequency needed. As it is necessary to preserve 110 Hz, these trace densities are not unrealistic. An excellent example of the preservation of high frequencies by fine spatial sampling and high trace densities (~ 850 000 traces /km^2) has been presented by Wood (1999).

Probably the most difficult challenge is to overcome the effects of the lignite layer. The high trace density will improve the signal-to-noise ratio for the data below the lignite layer, and as stated above, the use of a non-linear sweep may also be used to enhance the signal to noise ratio at the higher frequencies. Attenuation of the multiple energy will be improved by obtaining good offset sampling and by the high trace density. However, the actual amount of attenuation possible with the use of pre-stack multiple attenuation algorithms is very difficult to predict or calculate, without having field data on which to test the algorithms. The amount of attenuation possible from the effects of CMP stack can be simulated by the creation of a simple multiple model using the primary and multiple velocities from the velocity semblance plot provided.

After consideration of all of the above issues, several potential design geometries were created and synthetic trace data sets generated for the offsets corresponding to each of the different designs. Data sets were created for primaries only, and for primaries plus the main sequence of multiples. These were then processed and analysed to review the interference of the multiple energy with the primaries for the different geometries. This then allowed the selection of a final recommended design that gave the least multiple interference on the primary reflections.

Selected design

The basic template for the selected design is shown in Figure 2.

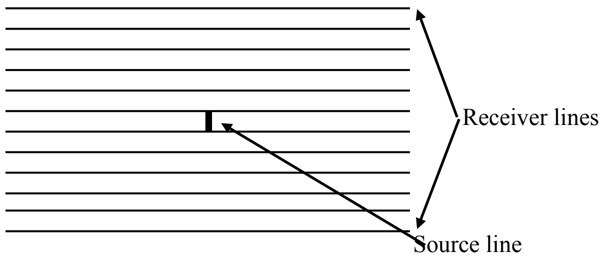

Figure 2 *Template for selected geometry. The geometry has 12 receiver lines with 320 receivers per line, giving a total of 3840 active receivers per vibrator point. The source and receiver lines are orthogonal, with spacing of 250 m and 400 m respectively. The source and receiver intervals are 25 m.*

Figures 3, 4, and 5 show the fold plots (for 12.5 m square bins) for offset ranges from 0 to 2000 m, 3000 m and 4000 m respectively. These approximate the offset ranges expected to contribute to the shallow, middle and deep targets. It can be seen that there is a relatively small spatial variation in the fold.

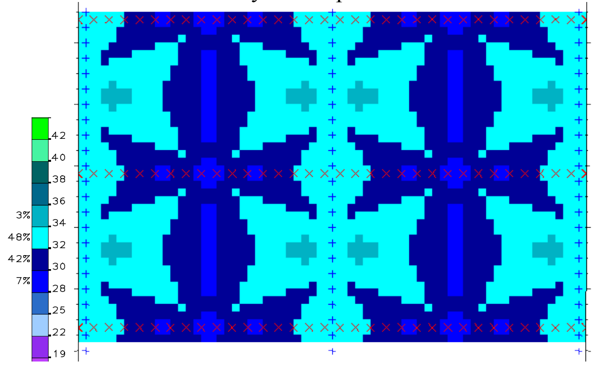

Figure 3 *Fold plot for offset range 0 - 2000 m*

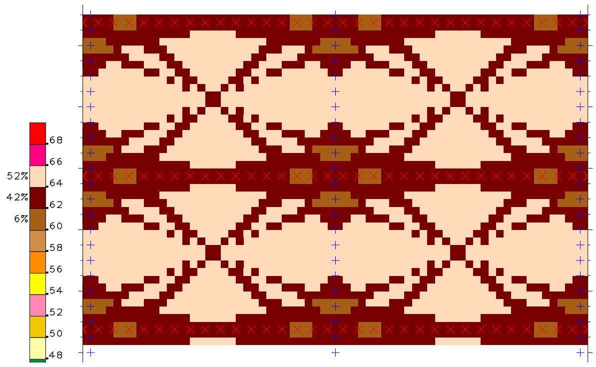

Figure 4 *Fold plot for offset range 0 - 3000 m*

The fold in 12.5 m x 12.5 m bins and the resulting trace densities for the different targets are:

Offset range	Fold	Trace density (traces/km^2)
0 - 2000 m	29 - 33	~201 000
0 - 3000 m	61 - 65	~406 000
0 - 4000 m	87 - 92	~573 000

For the shallowest horizon of interest this is within the range desired but on the low side, while for the deeper horizons they are greater than the desired range calculated earlier. Again, this should help with obtaining an adequate signal to noise ratio at the frequencies of interest.

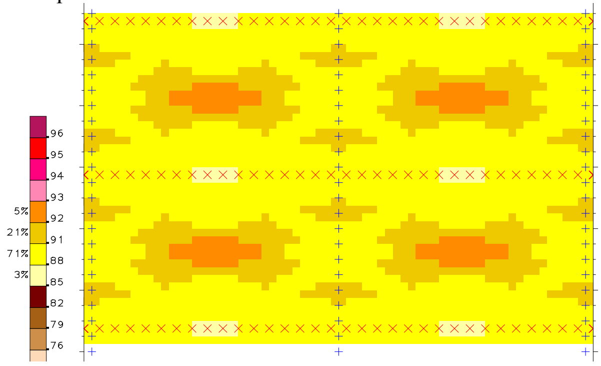

Figure 5 *Fold plot for offset range 0 - 4000 m*

The cost model and operational considerations

There are a number of issues with respect to the cost modelling equation. First, there is a great non-linearity in the equation as the number of recording channels approaches 3600, for which I see no theoretical reason. Costs most certainly do not become negative as the equation predicts! Although the cost of surveys does increase to a certain extent with increasing numbers of recording channels, a more linear change is usually seen. In fact, in many cases the overall cost of a survey frequently decreases with an increased number of recording channels.

A considerable number of surveys have been recorded on land with numbers of recording channels close to and exceeding 3600. These have been recorded quite efficiently and without this exponential increase in cost. A more reasonable estimate of costs was therefore generated which is very comparable to the original equation at the smaller number of recording channels, and which it is believed is more realistic for a greater number.

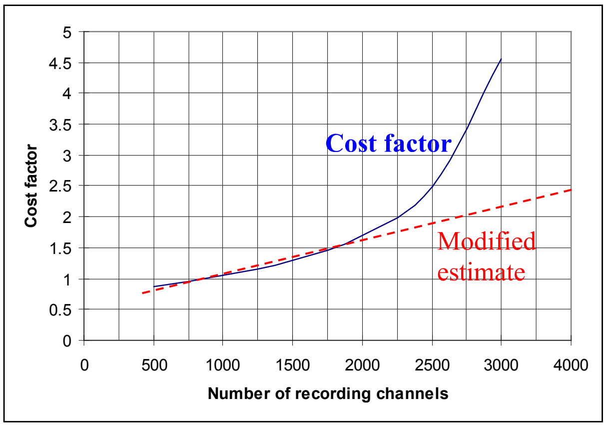

Figure 6 *Graph of the cost escalation plot for 6 geophones per group with the modified estimate added*

For 6 geophones per group the modified cost estimate was 2.3, while for 3 geophones per group the estimate was 1.75.

The second issue concerns the orientation of the receiver lines. If the receiver lines were to be laid out in the East-West direction, then the overall surface area will be approximately 10% larger than if they were to be oriented in the North-South direction. Similarly, the total number of source and receiver locations is also increased as shown below:

Survey statistics

	Receivers N-S	Receivers E-W
Surface area	495 km^2	547 km^2
Full fold percentage	71%	65%
Number of sources	79 095	88 130
Number receivers	50 135	54 641

However, from the operational standpoint, there will be some efficiencies to be gained from aligning the receivers in the East-West direction, since the overall number of cables and receiver groups required will be reduced, and the actual cost may be less, despite the additional field effort. Figure 7 shows the fold plot for the full survey area with the receiver lines oriented in the East-West direction.

Thirdly, there is no factor in the cost equation for the number of lines to be rolled in the crossline direction. From a geophysical perspective, a single line roll will give the most uniform attribute distribution. Since the cost-factor equation does not take account of variations in the crossline roll, all of the geophysical attributes shown have been calculated using a single-line roll. From an operational view, a multi-line roll should be more efficient. Therefore, although there is not a theoretical advantage according to the cost equation, the use of a multi-line roll rather than a single line roll should be evaluated for the impact on both the cost and geophysical attributes.

Finally, there is no factor for the sweep effort (the sweep length multiplied by the number of sweeps per vibrator point) in the equation. Since in my solution there has been a reduction in the number of vibrators, there should be an increase in the required sweep time per vibrator point, as stated earlier. This would result in the actual cost differential being greater than that predicted by the cost equation. However, many times it can be observed that the vibrator effort used on a survey is greater than is really necessary for signal to noise purposes. For this reason, the required sweep effort should be very carefully evaluated during the crew's initial field start up tests. When this is being done, it is important to remember that doubling either the number of sweeps or the sweep length gives only a 3 dB increase in signal to random noise (Lansley, 1992) and that it is very difficult to observe a 3 dB change in random noise.

Conclusions

In the design of this survey, the resolution requirements and the multiple problems caused by the lignite layer were deemed to be the more difficult issues with which to contend. A high trace density survey with fine spatial sampling and good offset distributions is required. In order to achieve the necessary high frequencies, small arrays at both source and receiver should be used.

The primary goal was to design a survey that would meet the geophysical objectives rather than to "design to cost." It is important to remember the quote (original author unknown) that has been stated many times: "The most expensive survey is the one that does not meet your objectives."

If the required high frequencies are not evident upon completion of the field evaluation of the initial tests, then the contractor should discuss with the oil company representatives the option to either abandon the survey, or to continue with reduced expectations for the resolution that is achievable. If this course of action is taken, then the cost benefits of the improved structural image of the 3D survey (with less than optimum resolution) can be evaluated.

References

Claerbout, J. F., 1985, Imaging the earth's interior: Blackwell Publications, 18.

Denham, L. R., and Sheriff, R.E., 1980, What is horizontal resolution?: 50th Annual Internat. Mtg., SEG, Reprints, paper G17.

Deregowski, S., Bloor, R. and Koeninger, C., 1997, Increasing Lateral Resolution, 59th EAGE Convention, Geneva, 1997

Embree, P., 1978, Rules of thumb for acquisition design: Presented at the EAEG Convention, Dublin, Ireland, 1978.

Embree, P., 1985, Resolutions and rules of thumb: Seismic Field Techniques Workshop, Monterey, California (August 1985).

Ebrom, D., and Lu, L., et al., 1995, Bin spacing in land 3-D seismic surveys and horizontal resolution in time slices: *The Leading Edge* 14, no. 1).

Krey, Th.C., 1987, Attenuation of Random Noise by 2-D and 3-D CDP Stacking and Kirchhoff Migration, Geophysical Prospecting 35, 135-147.

Krohn, Christine E., Rice, J.A., and Houston, L.M., 1991, Shallow Near-surface Effects on Seismic Waves: Presented at the 61st Annual International SEG Meeting, Houston, 1991

Lansley, R.M., 1992, Reducing the cost of land 3D surveys: Presented at the Vibroseis workshop, 54th Annual EAEG Meeting, Paris, 1992.

Vermeer, G. J. O., 1996, Factors affecting spatial resolution: Presented at the 66th Annual International SEG Meeting.

Widess (1982) Quantifying resolving power of seismic systems, Geophysics, Vol. 47, No.8

Wood, Paul, et al, 1999, Seria high resolution 3D survey revives the fortunes of a mature oil field: Presented at the 69th Annual International SEG Meeting. (Abstracts, page 1418)

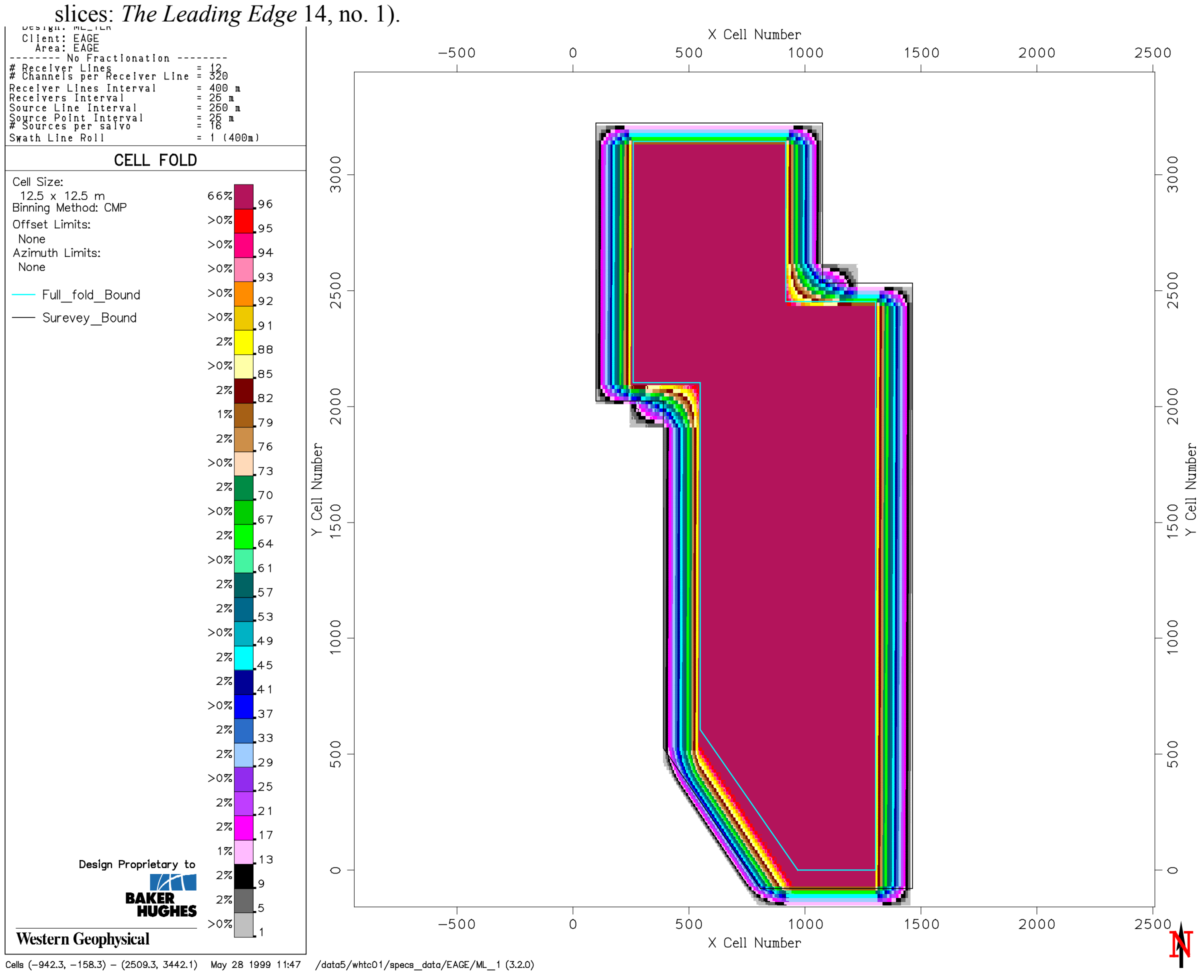

***Figure 7** Fold plot for the full survey area with the receiver lines oriented in the East-West direction.*

3D Seismic Survey Design: a solution by

J.Meunier and E. Gillot, *CGG*

Introduction

The following 3D-design analysis follows 2 basic principles:

- Keep operations as simple as possible.
- Rely on existing data as much as possible

The proposed solutions are described in Figure 1. We then present our analysis with particular emphasis on the few points that we think are not conventional.

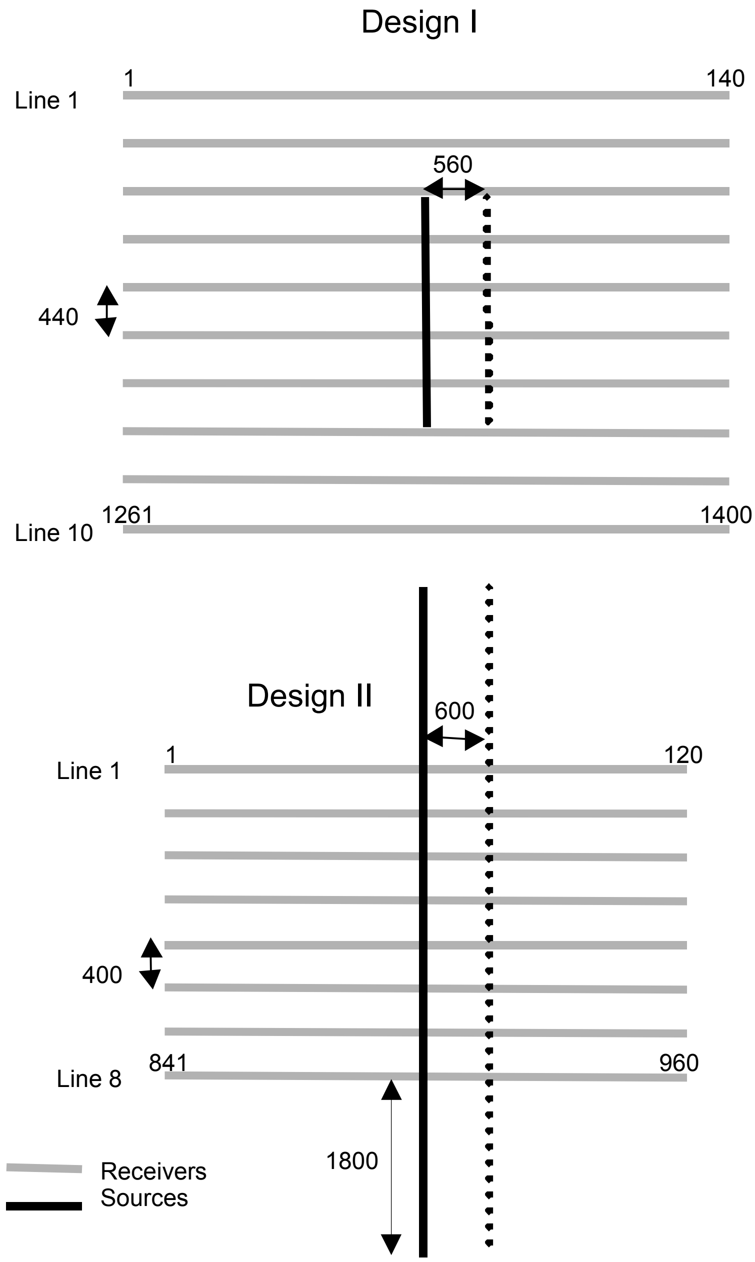

Seismic parameters	Design I	Design II
General		
Bin size (m)	20*20	25*25
Fold	25	40
Maximum offset (m)	4134	5458
Largest min. offset (m)	684	686
Swath overlap	5	0
Number of swaths	19(E-W)	6 (N-S)
Number of SP	21351	32970
Number of receivers	27050	24972
Cost factor	0.77	0.74
Source		
SP interval (m)	40	50
Line interval (m)	560	600
Number of SP/salvo	55	128
Number of SP/km2	44.64	66.67
Number of vibrators	4	2*4
Peak Force (kN)	229 kN	229 kN
Vibrator interval (m)	15m	15m
N sweeps/VP	1	1
Start frequency (Hz)	6	6
End frequency (Hz)	72	72
Sweep duration (s)	30	24
Sweep type	linear	linear
Receiver		
Station interval (m)	40	50
Line interval (m)	440	400
N lines/swath	10	8
N receivers/line	140	120
N receivers/km2	56.82	50
Number of channels	1400	960
N geophones/station	18	24
Distribution	3 lines	2 lines
Xgeo interval (m)	6.67	4.17
Ygeo interval (m)	10.00	7.5

Figure 1 -Proposed solutions

Source Parameters

Signal/Noise analysis: Source energy requirements are evaluated through an analysis using a frequency dependent Signal Strength Estimate (SSE) representing the amplitude of signal emitted at a given frequency and illuminating a surface unit. It includes the effect of noise, which is considered random. At any given frequency, signal amplitude in a bin is proportional to the number of vibrators, the peak force, the drive, the number of sweeps, the fold and the time spent shaking this frequency (this time is the inverse of the time derivative of the frequency law). Noise amplitude is proportional to the square root of the number of sweeps, of the fold and of the time spent. In a surface unit (3D) or length unit (2D), the signal amplitude is divided by the bin area (3D) or cdp interval (2D), the noise amplitude by their square root. SSE is expressed in kN.sec /$m^{1/2}$ in 2D and in kN.sec /m in 3D.

$$SSE = N_v * P_f * D * \sqrt{\frac{N_s * C}{b}}\sqrt{\frac{dt}{df}}$$

For a linear sweep, it becomes frequency independent (within the sweep range):

$$SSE = N_v * P_f * D * \sqrt{\frac{N_s * C * SL}{b * SR}}$$

N_v = number of vibrators
P_f = Peak Force (kN)
D = Drive
N_s = Number of sweeps per VP
C = Fold
df/dt = time derivative of the frequency law
SL = sweep length (s)
SR = sweep range (Hz)
b = bin size (2D=m 3D=m^2)

SSE can be used to compare 2 or several acquisition designs: The ratio of their respective SSE directly represents S/N ratio improvement (or degradation). One difficulty is when the comparison involves existing 2D and proposed 3D data (in which unit should the bin size be expressed?). A way of relating 2D and 3D data S/N ratio is by considering the difference between them as an extra 2D migration (assuming there is a constant velocity field). This extra migration conserves the amplitude of reflections and modifies the amplitude of non organised noise. This modification is a function of time, frequency and bin size. Figure 2 shows the amplitude variation of white noise migrated with the appropriate velocity field in 3 time windows corresponding to the 3 targets and using 20 or 25 m bins as measured on synthetic data.

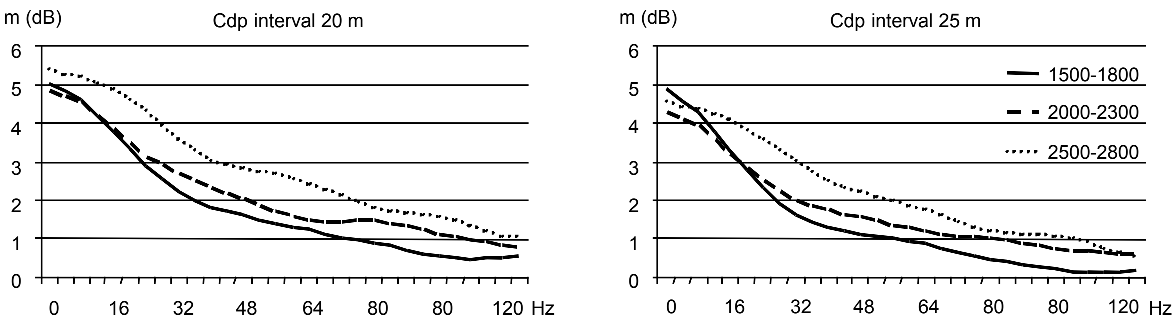

Figure 2 –Modification in Signal/Noise ratio by 2D migration.

Our indicator becomes:

$$SSE_m = m * N_v * P_f * D * \sqrt{\frac{N_s * C * SL}{b * SR}}$$

where b is the cdp interval in 2D and the inline bin length in 3D,
and m = 1 in 2D and is given by the above curves in 3D.

Taking the selected source parameters, stacking fold, bin size and m factor into account, the resulting theoretical modification in S/N ratio relative to line A is given by the following table. For example the S/N ratio after migration obtained with design I at 60 Hz is 5.2 dB below the S/N ratio of line A.

	Design I			Design II		
	20 Hz	40 Hz	60 Hz	20 Hz	40 Hz	60 Hz
1500-1800 ms (Main Target)	-3.2dB	-4.7dB	-5.2dB	-3.6dB	-5.1dB	-5.5dB
2000-2300 (Mid-Syn-rift)	-3.0dB	-4.2dB	-4.9dB	-3.6dB	-4.7dB	-5.1dB
2500-2800 ms (Near basement)	-1.9dB	-3.5dB	-3.9dB	-2.6dB	-3.9dB	-4.5dB

The poor quality in the target areas on line A does not justify a decrease in S/N ratio. However, we interpret this low quality as a result of inadequate (2D) migration and multiple interference.

<u>Frequency range:</u> Analysis of line A shows that despite an 8-80 Hz sweep and adequate array filtering (50-m source and 20-m receiver arrays), no significant energy is present above 60 or 65 Hz at the main target level. There is no reason to hope that in a future 3D survey, higher frequencies can be obtained. Therefore, the desired 14-m vertical resolution may not be fully achieved. Low frequencies are certainly needed to image the deeper targets. The low velocity of the noise will allow a large proportion of useful data to be observed at these frequencies. We propose a [6-72 Hz] linear sweep with a low end taper allowing a smooth sweep start.

<u>Spatial distribution:</u> The noise velocity in the area is less than 500 m/s. Any station interval above 20 or 25 m will not allow effective noise reduction by velocity filtering. In these conditions, honouring anti-aliasing criteria in the cross-spread domain (array length = station interval) is of secondary importance. Therefore, we propose a vibrator array with an interval compatible with fast operations: 15 m resulting in a 60-m array for both designs far enough below the 90-m wavelength notch associated to a frequency of 65 Hz reflected on the deeper target and observed at a 3000-m offset.

<u>Sweep length</u>: Set at 30 s (design I) or 24 s (design II) by the above S/N analysis.

Receiver Parameters

<u>Geometry</u>: It is unlikely that a geophone interval lower than 6 or 7 m shows a significant advantage in the reduction of either ground-roll (which does not show significant energy at wavelengths around these values) or natural noise. We have selected 18 geophones per station for design I, in 3 lines of 6 with a 6.67 m separation in X and 10 m in Y and 24 geophones for design II in 2 lines of 12 with a 4.17 m separation in X and 7.5 m in Y.

<u>Geophone frequency:</u> Standard 10 Hz geophones are adequate to record data in the selected frequency range (6-72 Hz).

Recording geometry

<u>Bin size</u>: it is determined by the non-aliasing condition of the highest expected frequency on the main target.

$$b < V/4f_{max}\sin a$$

with 2500 m/s, 65 Hz and 20°, $b < 28$ m

Although strictly acceptable, a 25m-bin size seems a little close to the limit. We think a 20m bin is more appropriate. This is why we propose 2 solutions. An evaluation of the appropriateness of these bin sizes is provided by a 2D migration of existing 2D data with the proposed bin size.

<u>Offset/azimuth distribution</u>: Multiple reflections associated with the lignite layer will interfere with the reflections for at least the upper two targets. A wide azimuth geometry provides an offset distribution which is favourable to multiple attenuation (there are more longer offsets). We think this characteristic should be taken advantage of. Design I uses a wide receiver patch (3.96 km), design II uses a cross-spread. Since the survey width would impose a very large number of stations on the ground to avoid geophone redeployment with a 10-line geometry with full overlap (~ 4000), we propose, for design I, to use a 50% overlap which lightens the burden on geophone deployment while marginally degrading offset distribution.

Maximum offset: An angle of incidence of 30° on the deeper target (at 3600 m and horizontal) corresponds to a source-receiver offset of 3000 m. The offset distribution of our proposed solutions is maximum around this offset.

Minimum offset: Although the strong lignite reflectors at about 1s are not of primary interest for the interpreter, they will be extremely useful for the processor (for instance to compute and evaluate residual statics). It is therefore important to properly image these reflectors. It is also relatively easy. Relatively large line intervals (500-600 m) will be acceptable: Figure 3 compares 3D stack simulations with a 2D stack simulation using a single (2D) CMP. Such a simulation could have been done using a complete 2D line. It would have produced a more realistic picture and it would enable some further Signal/Noise ratio analysis. In this particular case, the 2D CMP is in fact a shotpoint. Therefore, the simulation validity is restricted to horizontal reflections (above all targets). In these conditions, it only provides an evaluation of the image degradation in the bin with the largest minimum offset. In our case (684 and 686 m), it is not a marginal degradation; however, we expect that a thorough velocity and static analysis applied to a true bingather will significantly improve the image, making it fully acceptable.

Stacking fold: Set at 25 and 40 by the above S/N analysis.

Line orientation: With a wide geometry, geology does not impose any orientation preference and leaves the selection to operational constraints. With about 3000 stations available in the field it will be possible to record E-W swaths using design I without significant geophone re-deployment. Depending on local conditions, it may be more convenient to record long swaths with about half this amount of stations using the cross-spread geometry of design II.

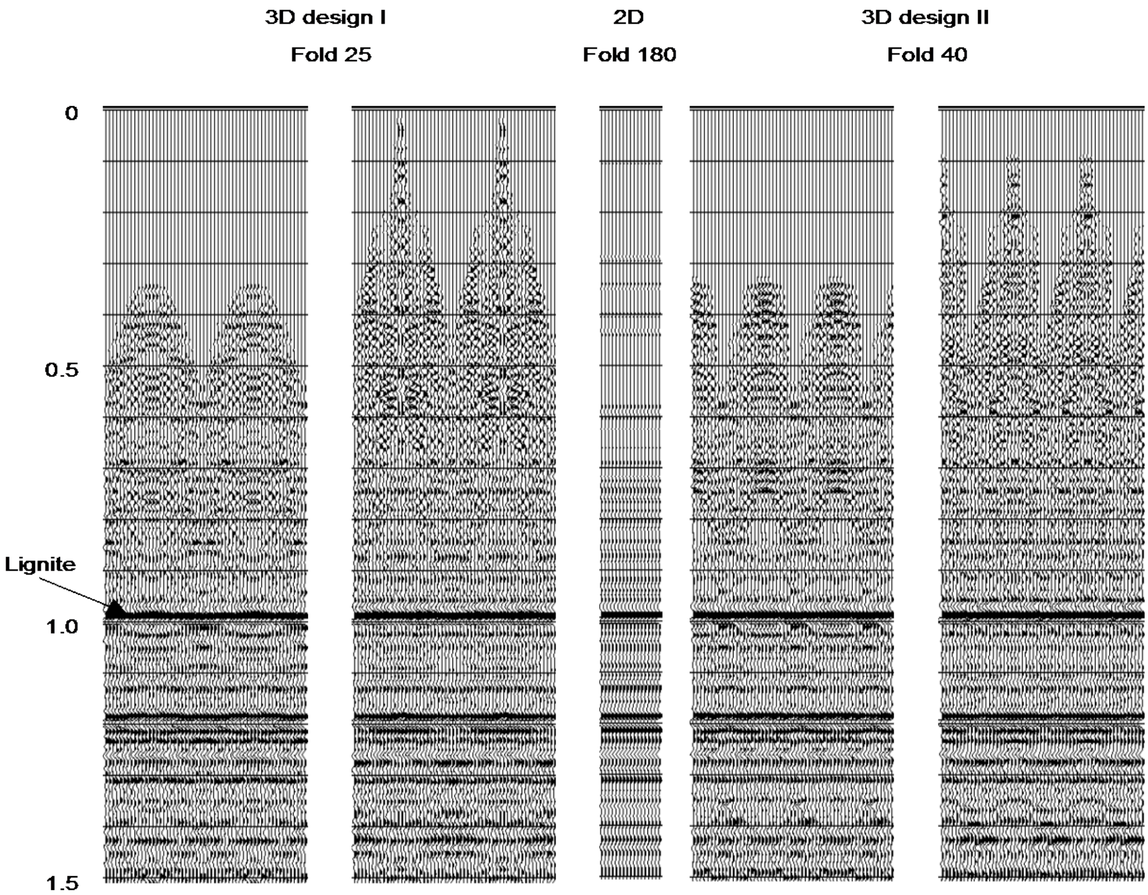

Figure 3 – Comparison between 2D and 3D stack simulations. For each 3D design the right panel represents a section above a receiver line, the left panel a section between receiver lines.

3D Seismic Survey Design: a solution by

Dave Monk (*Apache Corporation*) and Mike Yates (*Continuum Resources*)

some more questions and answers

Introduction

Through the luck of the draw, this paper was presented last at the workshop. This was perhaps the most suitable place for some of our comments which suggested that the workshop exercise mimicked the real world in supplying an underspecified problem. Our expectation was that most participants would suggest different solutions, and we tried to answer the question of what additional information might have drawn these solutions together.

In a recent paper (Liner and Underwood 1999) 3D survey design was described a two-step process. In our workshop presentation we concentrated on the first step, that of "pre-design". Pre-design is a stage of analysis based on geophysical, practical and financial issues which lead to the establishment of fundamental criteria for acquisition before the second step of survey design (establishment of geometry and shot and receiver positions) can be started. The inputs to the pre-design stage are all available data and information, and the outputs are the geophysical parameter requirements to optimise target imaging. Integration of the knowledge gained in pre-survey analysis step allows a workable survey design to be constructed, and we illustrated our results by generation of an example survey geometry. We hoped to show that our example geometry was neither a unique or perhaps even the most appropriate solution.

If indeed the problem posed for this workshop had had a unique geometry solution, then it should be expected that each of the participants would find the same answer. However, in fact there are enough unknowns that problem is under-constrained and open to interpretation, and all workshop participants suggested a different solution. While the workshop organisers had gone to reasonable lengths to supply background information, they had in fact missed some critical data from the problem description, only hinted at other information, and on occasions (perhaps deliberately to increase the non-uniqueness of the solutions) given somewhat misleading information. This actually made the workshop exercise more realistic. Examples of each might be:

Missing Information- location of the survey, survey design might be influenced by crew availability and local terrain in a geographic area.

Hinted Information- Survey area is described as being in a "reasonably densely populated" area. Does this mean there are roads? Would roads lend themselves to alignment with receiver or shot-lines? Are there areas where recording or shooting cannot go?

Misleading information- The survey outline is supplied in terms of a "full fold boundary". Unless the workshop organisers have already completed the design, then they could not have known the layout geometry, and therefore did not know the full fold boundary. Should this be "required full image boundary", "maximum permissible surface extent" or some other bounding feature? Very different survey sizes may result from this ambiguity.

These and other variables should (and did) lead to a dynamic comparison of the various solutions which were offered at the workshop, and led to some interesting debate. We hope the "solutions" offered here to some of the pre-survey design problems helped participants understand some of the important criteria for 3-D survey design, and predict that there will be many variations proposed for the basic parameters affecting resolution: Aperture; Geometry; Fold and Sampling (Vermeer 1998).

Basic information

Much of the basic geologic requirement data is stated in the cover sheet to this workshop paper, and as such is not repeated here.

Some of the missing information

We knew from the description of the project that both structure and stratigraphy are important, but there are still some unknowns, both in geologic objective and intent for the data usage. While amplitude information is obviously important, without doing a detailed modelling study we would not know (for example) if pre-stack amplitude information (AVO) is useful in this data. Some additional missing information and related questions to ask of the geologist in the project might be:

1. Is AVO of interest?
2. Are azimuthal variations expected to be indicative of useful reservoir information?
3. Is pre-stack time or depth migration intended, which may require different spatial sampling?
4. Is there a possibility of useful shear wave signal? Should the survey be designed to utilise 3 component 'phones?
5. Is there potential for 4D (repeated seismic) studies requiring later repeat surveys of the area, which would impact the choice of design parameters?

We have in our approach assumed that in general it is the intent that the data be processed through a conventional DMO, Stack, and Migration process to be interpreted post migration. The answer to all the questions above is therefore assumed to be "No!" However, we stress that if the answer to any or all of the questions is "Yes", then the resultant survey design would almost certainly be different.

Some fundamental questions to be answered:

1. *How big does this survey need to be?* Many 3D surveys fail through misunderstanding of the boundary requirements. Would you design a 3D survey to tie seismic to well data, and have the well on an edge CDP from the survey? Without first establishing the desired image area at the target the final survey area cannot be established. 3D Surface area is greater than full fold area, which is greater than fully imaged area, which is smaller at later times.

2. *What is the true population density, and what kind of agriculture dominates this area?* On a featureless target map, a source and receiver layout can be made to meet the geophysical requirements, satisfy budgetary needs and fit over a polygonal outline, but drop that layout over a local topographic map and the fit may disappear. What is the predominant alignment of the dunes dominating the area? Is there a pattern to the local road or track network that would provide a logical "path of least resistance" for source or receiver lines? Are there climatic or agricultural issues that will affect the execution and cost of the survey in terms of standby or permit costs?

Pre-design parameter determination

Our focus is on some of the fundamental pre-design criteria and parameters. There is of course a fundamental dilemma in 3D survey design in that technical impetus is exactly opposite to the financial impetus. This is illustrated in the following table:

Survey Impetus	**Cost Drivers**	**Technical Drivers**
Survey Size	Small as possible	Big as possible
Sampling (spacing)	Coarse	Tight
Sampling (Fold)	Low	High
Offset Range	High min, Low Max	Zero-Long
Azimuth Range	? (whatever is cheapest)	All (with all offsets as well!)

All designs are therefore based on some level of compromise, and it is important that acceptable compromise be reached both technically and financially. In our approach to survey design, the initial geophysical information is studied by input into a generic set of formulae which allow analysis of the various compromises. Input information for this study is of the form:

Objectives - EAGE Helsinki Workshop				
Minimum Dip (deg) to be Imaged		**0**	Maximum Structural Dip (deg) imaged	**20**
Minimum Objective Depth		**2300**	Maximum Objective Depth	**3000**
Time in s of Minimum Objective Depth		**1.90**	Time in s of Maximum Objective Depth	**2.50**
Minimum Offset Required for figures		**2000**	Maximum Offset Required for figures	**3500**
Dominant Seismic Frequency Expected		**30**	Maximum Diffraction Distance to Migrate	**3000**
Minimum Seismic Frequency Expected		**10**	Maximum Seismic Frequency Expected	**60**
# of Spatial Samples / cycle (n)		**2**	Minimum Bin Interval to use	**10**
Minimum RMS Velocity at Objectives		**2480**	Maximum RMS Velocity at Objectives	**2589**
Minimum Interval Velocity at Objectives		**2803**	Maximum Interval Velocity at Objectives	**2911**
Velocity Function, V = Vo + kZ	**2000**	**0.50**	Required Spatial Resolution, e.g. faults	**200**
Max allowable NMO stretch factor		**30%**	"1" for RMS or "2" for Interval Vel	**1**

Using these input parameters it is possible to determine some of the fundamental geometry requirements such as:

- Migration Aperture
- DMO Aperture
- Sampling (CDP) interval
- Offset mute patterns, and
- Maximum offset requirement.

Some of the parameters are:

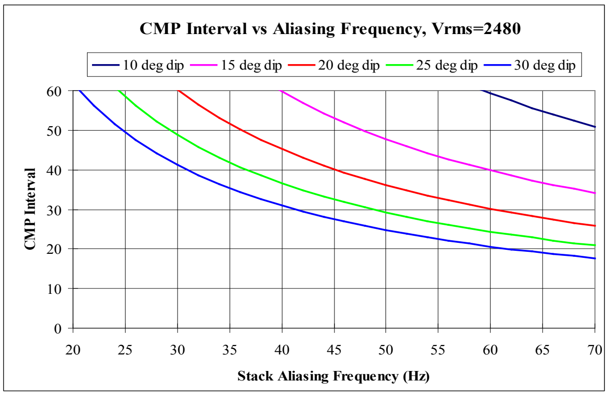

Figure 1: Bin size determination

Subsurface Sampling – From target depth, dip and velocity information it should be possible to record unaliased signal up to 60 Hz from events dipping up to 20° using a subsurface bin interval of 30 m. If an acquisition crew with 30 m group capability is not readily available (and would therefore be associated with an increase in cost), a 25 m interval would only improve survey capability. Figure 1 shows the compromise between dip, alias frequency and bin dimension (sampling interval).

Maximum Offset – From velocity information, seismic data analysis and assuming that a conventional 30% NMO stretch is a reasonable limit for useful data on long offsets, a maximum offset of 3500 m enables capture of all useful reflected energy at primary target depths. Of course if AVO is of interest, and/or more stretch of events at longer offsets can be tolerated, then it is possible that longer offsets may be useful.

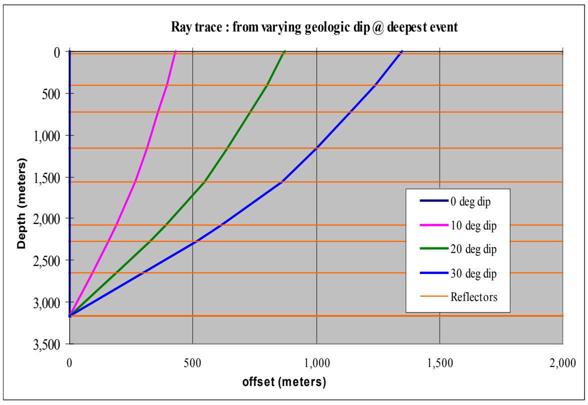

Figure 2: Ray traced migration aperture example

Migration and DMO Aperture – Velocity and Dip information lead to a model-ray migration aperture of approximately 1280 m, plus a DMO Aperture of approximately 300 m that must be added on some sides of the desired image area. Note that Liner and Underwood (1999) stress the importance of performing this calculation and accounting for velocity gradients. In our approach, we examine the constant velocity situation, the gradient solution, and a modelled ray trace approach which can be useful in examining the fit of a gradient approach. Figure 2 shows a ray traced aperture illustration for different dips through a layer cake subsurface in the presence of velocity information. The curvature to the rays is very similar to that found with a constant gradient approach, and in fact the migration apertures computed this way are similar, which is not surprising given that the interval velocities show reasonable agreement to a smooth gradient function (see Figure 3).

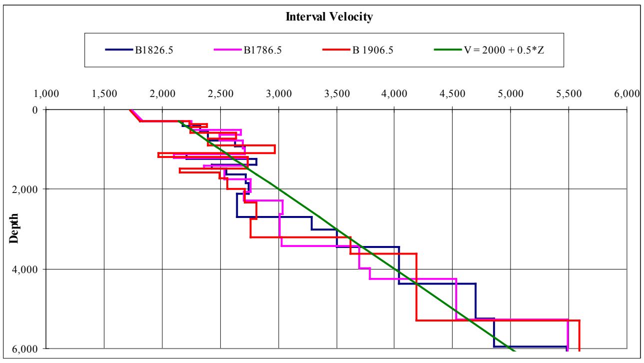

Figure 3: Interval velocity functions derived from Line "B"

In case the reader is in any doubt about the potential costs and savings in doing this computation correctly, it should be noted that the aperture computed using straight rays for this study is approximately 1750 m. Curved and model ray analysis reduces this by about 450 m. A 450 m "fringe" around the survey area would add approximately 40 km^2 requirement to the survey area. Assuming just over \$10 000 / km^2. (we have no basis for this number as there is no information about location or crew availability), this would add close to \$500 000 to the acquisition cost.

DMO aperture is often forgotten, but can have a significant impact on the survey size and orientation. Migration apertures are usually computed for zero offset data, but finite offset data has a Fresnel zone which is elongated along the shot receiver axis. DMO collapses this elongation in addition to other corrections. In this survey the DMO aperture computation would lead to approximately 300 m additional aperture being required in some directions.

Seismic data

In the study information data set, the workshop organisers supplied examples of 2D seismic from the survey area. Existing seismic data is invaluable in designing a 3D survey. It allows much better understanding of (for example) offset requirements, statics issues and S/N in the area. Using this data it was possible to verify some of the fundamental parameters previously established, and also to make recommendations on minimum offset and required Fold of coverage. From processing tests carried out with data provided, a minimum offset of 600 to 800 m was found to be adequate without significant image degradation at target (if stacks were produced with no data of offset less than 600 m, and compared to full offset stacks, the difference was negligible). Additional processing tests indicate that 2D fold of 28 to 32 enables imaging of the target without significant signal to noise compromise. The inherent S/N improvement of the 3-D process will offer further improvement, and provide the survey some resistance to fold drops due to obstruction.

Survey dimension and layout

Choice of receiver line direction can greatly impact the final surface layout by governing the location of fold tapers. Laying lines parallel to the long axis of the survey may reduce the eventual surface area, but introducing zippers and the associated inefficiency in rolling spread may outweigh savings. Final determination of orientation cannot be made without information about surface obstructions and condition. However we would anticipate for the survey, that if receivers are laid along the long axis, the area will be approximately 420 km^2 and if laid along the short axis the area will be approximately 440 km^2. While it may seem obvious to lay receivers along the long axis of the survey (to reduce the surface area) this introduces "zippering" (40 km long lines = 800 x 50 m stations or 666 x 60 m stations) and thus increased operational expense. Laying along short axis results in lines approx. 12 km long (240 x 50 m or 200 x 60 m), which are easier to lay and roll, and therefore faster to shoot.

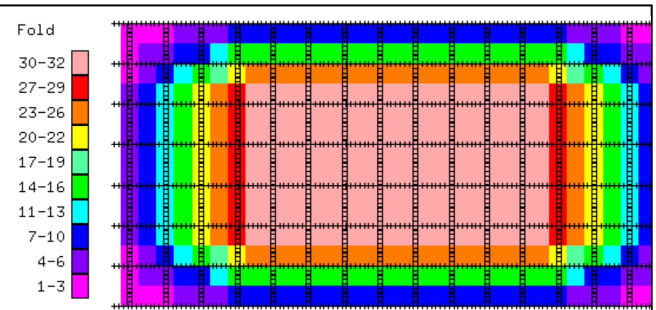

Figure 4: Nominal geometry layout

From the analysis performed in the pre-design stage, a receiver line interval of 540 m, and source line interval of 480 m, with 60 m spacing for both sources and receivers are recommended as reasonable compromises, with an active receiver template of 8 lines, each of 128 active stations. This template would satisfy the geophysical requirements of the survey, generating nominal 32 fold, with offsets from a maximum short offset of 700 m to a minimum long offset of at least 3700 m in every bin. Using the cost escalation formula provided, the above parameters result in a cost escalation factor of 0.66. The layout of source lines relative to receiver lines largely depends upon operational preferences and efficiencies in the area. While we propose a simple orthogonal template, we have no reason to recommend this compared to, diagonal, zigzag or other definitive source line technique.

Conclusions

In this short abstract we cannot satisfactorily cover all aspects of pre-survey design. Even though we have taken a minimalist approach to unknowns we have still not discussed aspects (for example) of noise attenuation, multiples and statics, and their influence on optimum design criteria. It was our expectation that other workshop participants would concentrate more on the second stage of survey geometry development, which follows the establishment of fundamental geophysical parameter requirements, an expectation which was more than amply met.

While our approach was minimalist, it did not generate the lowest "cost escalation factor" of the day, but was a long way short of the highest. While we do not necessarily condone the attitude that "cheapest is best" we do acknowledge the need for geophysically, environmentally and economically responsible approaches to 3D problems. We feel that having seen the proposals of the other contributors to the workshop we believe that our solution was simply one of many possible answers, but maintain that the information provided was only sufficient to initialise this project and define basic geophysical requirements for this undisclosed area. In a real world case the additional information obtained in response to our unanswered (and in this case unasked) questions would, in combination with local client and contractor experience, enable the selection of economically realistic, geophysically sound parameters for the solution of this exploration problem, and the various solutions proposed would have converged more closely.

References

Liner C.L., and Underwood W.D., "3-D seismic survey design for linear v(z) media", (1999), Geophysics Vol. 64, No. 2.

Vermeer G.J.O., "Factors affecting spatial resolution", (1998) The Leading Edge August.

3D Seismic Survey Design: a solution by

James A. Musser, *GMG Energy Services*

As with all 3-D seismic design problems, the proposed solution to this imaging problem will involve multiple compromises between geophysical parameters and operational costs. The objective of this paper is to present a suitable survey design with parameters that can meet the geophysical interpretation goals cost-effectively.

Geophysical Calculations and Issues

To estimate the relative importance of various geophysical parameters for evaluating compromises, a number of formulae are used and discussed below for calculating seismic acquisition parameters from known properties of the geophysical objectives. These calculations include bin size, minimum far offset, and resolution.

Because of the expected statics problems caused by the dunes, the complexity of imaging in all directions, and the surface obstructions expected due to culture, surface consistent statics coupling and wide azimuth data distributions will also be important factors in the survey designs. These problems will make the selection of appropriate processing algorithms, such as coherent noise attenuation, 3-parameter velocity analysis, 3-D DMO, and 3-D migration very important.

Bin Size (subsurface sampling)

Anti-aliasing calculations for bin size are typically based on the simple formula:

$$dX_{subsurface} = V_{avg.} / (4 \times f_{max} \times \sin(\alpha_{max})), \qquad (1)$$

where $dX_{subsurface}$ is the subsurface CDP bin size, $V_{avg.}$ is the average seismic velocity to the target reflector, f_{max} is the highest unaliased seismic frequency in the wavelet, and α_{max} is the maximum dip to be imaged without aliasing. In general, lower velocities, steeper dips, and higher frequencies will require smaller bin sizes for adequate spatial sampling of the higher frequency signals. For the seismic velocities, dips, and frequencies expected, the resulting bin size is about 27 m, using an average seismic velocity of 2450 m/s, maximum dip of 20^o, and maximum unaliased frequency of 65 Hz.

However, the structural dip of the target beds is not the only dipping seismic signal that must be accurately recorded. Faults will cause truncations on beds that will generate diffraction events with apparent dip that can be significantly steeper than the structural dip of the horizons. Because of faulting and the target complexity, I recommend designing for a 30° dip to capture adequate energy from the diffractions to image the faults without spatial aliasing. Using the same velocity as above, this will result in a recommended bin size of 20 m. In conventional mid-point analysis, the subsurface sampling interval is one-half the source and receiver sampling at the surface. Therefore the surface receiver group and shot intervals should be 40 m. Using a bin size of 20 m will allow unaliased frequencies of up to 90 Hz to be recorded from beds dipping at 20^o.

Offset Requirements

The long offsets required in a survey are determined by velocity, multiple attenuation and AVO considerations. Through algebraic manipulation, the Dix hyperbolic normal moveout equation, which relates offset, X, normal moveout velocity, V_{nmo}, two-way zero-offset travel time, t(0), and moveout time, Δt, can be rewritten as:

$$X = V_{nmo} \times \{\Delta t^2 + 2 \times t(0) \times \Delta t\}^{1/2}. \qquad (2)$$

In this form, to solve for the long offset, a value for Δt is selected that will allow a stable determination of the velocity. In many cases with a good seismic wavelet, a temporal moveout across a CDP gather (Δt) of 200 ms is reasonable for accurate velocity analyses. In order to have 200 ms of normal moveout on the deepest target reflection event (in this case with t(0) = 3.0 s and V_{nmo} = 3000 m/s), the long offset should be about 3300 m.

These long offsets are important for overcoming the multiple problems associated with the velocity inversion caused by the lignite layer. Longer offsets will enable more accurate velocity determination and better multiple attenuation. Conversely, shorter long offsets would lead to less accurate velocities and less multiple attenuation. For these reasons, the minimum long offset from the 3-D design should be on the order of about 3000 m.

Near offsets are determined by the need for shallow data. In this survey area, the shallow data are not critically important to the interpreter, but they are important for solving residual reflection statics. As the near offsets are controlled by the source and receiver line densities, reducing the near offsets significantly requires decreasing the source AND receiver line spacings. That means more shots and receivers per square kilometre, and hence more cost. To balance the near offsets and the operations, a maximum near offset of about 600 m is desired to provide continuous subsurface coverage at a two-way travel time of about 400 ms in the stacked data.

Resolution

Vertical resolution of the thin sand bodies found in this survey area can be estimated from the interval velocity of the targets and the dominant frequency of the seismic wavelet using classic Rayleigh ¼-wavelength (¼-λ) resolution analysis. This type of analysis is based on the ability to resolve reflection events from the top and bottom of a layer. This can be written as:

$$\frac{1}{4}\text{-}\lambda = V_{interval} / (4 \text{ x } f_{dom}) , \qquad (3)$$

where $V_{interval}$ is the interval velocity of the target layer and f_{dom} is the dominant frequency of the seismic wavelet. For an interval velocity of 2760 m/s at the target and a seismic wavelet with a dominant frequency of 30 Hz, the ¼-λ resolution is about 23 m. In order to improve the vertical resolution to image the top and bottom of a sand body with a thickness of just 14 m, the wavelet must be improved to have a higher dominant frequency (and broader bandwidth to avoid ringing) of about 50 Hz. For a **dominant frequency** of 50 Hz, it is necessary for the seismic wavelet to contain unaliased frequencies of approximately 85 to 100 Hz. This illustrates the importance of maintaining the maximum possible frequencies in the seismic wavelet.

The anti-aliasing relationship that was used earlier to estimate the required seismic bin size (equation 1) can be rewritten to estimate the maximum unaliased frequency, f_{max}, at the target. The new form of the equation uses the interval velocity at the target, V_{int}, the bin size, $dX_{subsurface}$, and the maximum structural dip, α_{max}, as follows:

$$f_{max} = V_{int} / (4 \text{ x } dX_{subsurface} \text{ x } \sin(\alpha_{max})). \qquad (4)$$

As calculated above, with the proposed bin size for spatial sampling of 20 m, the maximum unaliased frequency expected is about 90 Hz for beds dipping at 20°. If such high frequencies can be recorded at the target horizon, it will be possible to resolve the dipping thin sand beds at the target. However, the source effort required to record such broadband data may be substantial and pre-survey testing would be required to determine the parameters needed to provide this data quality.

Statics Coupling

Cross-line statics problems can only be properly solved using wide azimuth acquisition techniques that provide surface and subsurface overlap between swaths and relatively long effective cable lengths (or offsets) in both in-line and cross-line directions. Statics coupling is enhanced by variations in shot and receiver positions. Shifts of shot and receiver locations to avoid obstacles in the field will cause mixing of the contributions of different shot and receiver pairs in the CDP bins. This mixing induces surface consistent statics coupling. Thus randomisation of positions caused by culture and topography is desirable and can yield geophysical and operational benefits.

In areas where surface shifts of sources and receivers are not guaranteed, statics coupling can be induced by using variable source and receiver line spacings, with line spacings varying by plus and minus one shot or group interval. For example, the receiver line intervals can be varied by plus and minus one shot interval (such as between 360, 400, and 440 m) with the number of shot points between the lines varying accordingly (in this case 9, 10 and 11 shots per salvo, respectively). In a similar manner, the shot salvo roll intervals can be varied by plus and minus one receiver group interval (for example, between 440, 480, and 520 m). When designed and rolled properly, shooting patterns with variable line spacing will maintain the fold and overall offset distribution of a normal orthogonal design, only changing the near offset distribution and mix of offsets within each CDP bin. It will also allow surface consistent statics algorithms to uniquely solve statics problems across the swaths without changing the shot and receiver density over the survey area. Variable line spacing will further smooth the offset distribution within each CDP bin and reduce the differences from bin to bin.

Survey Designs

There are basically four classes of survey design that can be considered for this project. They all have some similarities and some very important differences. The four classes of surveys are In-Line Swath, Orthogonal Swath, Brick Swath, and Slant Swath.

A Narrow-azimuth In-Line Swath design with short cross-line offsets cannot resolve cross-line statics. Operationally, this technique requires a high density of both shot and receiver stations, but it can be processed to a large degree using 2-D algorithms.

Industry-standard Orthogonal Swath designs can be used to efficiently and effectively collect wide-azimuth seismic data and can solve cross-line statics problems. Wider source and receiver line spacings can be used to minimise the source and receiver density to control operational costs. This technique also allows efficient undershooting of obstructions. However, in order to properly analyse and process the irregular, wide-azimuth data acquired with an orthogonal pattern, true 3-D processing algorithms, such as coherent noise attenuation, 3-parameter velocity analysis, and 3-D DMO, must be appropriately used. Because of the sparser grid of source and receiver lines, there are gaps in the near offset distribution and the overall offset distributions in many bins are not smooth. Such offset variations can lead to non-uniform noise attenuation and the appearance of "footprints" or artefacts in the processed data, especially visible on shallow time slices.

Brick Swath shooting patterns have the same advantages as orthogonal designs, with an added advantage of improving the near offset distribution and the overall smoothness of the offset distributions, making the "footprint" patterns in shallow time slices less obvious. However, in many environments, brick shooting can be more difficult for source operations because the source lines are discontinuous across receiver lines.

Slant Swath shooting is closely related to both orthogonal and brick shooting. In slant shooting the shot salvos form an angle (often 45° or 63.43°) with the receiver lines. The slanted shot lines improve the near offset distribution and smooth the variations in the offset distributions, reducing the severity of "footprint" patterns without any increase in shot point density. When designed properly, the shot lines are continuous across the receiver lines for more efficient source operations.

In all of the wide azimuth design types described above (orthogonal, brick, and slant), the variable line spacing technique for statics coupling can be used. This technique will further reduce offset variations and gaps within each CDP gather. When properly implemented, variable line spacing will acquire data with uniform fold coverage with continuous shot lines allowing efficient operations.

The recommended survey design is shown highlighted in black in Figure 1. It uses 10 active receiver lines each with 144 stations on 40-m group intervals to collect 30-fold data in 20-m square bins. Variable line spacing is used for surface consistent statics coupling, and slanted shot salvos help to improve offset distribution. The design collects wide-azimuth data with cross-line offsets nearly as large as the in-line offsets.

A detail of the near offset distribution in each CDP bin for the recommended design is shown in Figure 2. Using the same colour scale, Figure 3 shows a corresponding display of near offsets for an orthogonal design with the same nominal line spacings. These two figures show the improvement in the near offset distribution for the slant design. Note that the areas with large near offset (shown in pink, red, and orange) are wide and very regular for the orthogonal pattern in Figure 3, while they are quite narrow in Figure 2. With the slant design, a gather with a large near offset is never far from one with a significantly shorter near offset. Figures 4 and 5 compare the long offsets collected by the slant and orthogonal patterns, respectively. In both cases, the long offsets are about 2900 m or longer in every CDP bin, and larger than the design goal of 3000 m in the large majority of bins. However, in Figure 5 (for the orthogonal design), the areas with small far offset (shown in white, pink, and blue) are quite large and very regular.

The recommended slant design provides a smooth offset distribution with moderate offset gaps. This can be seen in Figure 6, which shows the distribution of maximum offset gaps between traces within each CDP bin. Note that the larger offset gaps occur at the intersections of source and receiver lines. Figure 7 shows the corresponding maximum offset gaps for the orthogonal design with the same colour scale. These plots show a measure of the smoothness of the offset distributions. Note that while there are bins with rather large offset gaps in both designs (shown in red), the dominant offset gaps for the slant are less than those for the orthogonal design, shown in Figure 7, and the patterns in Figure 6 are more dispersed. Note also the secondary pattern of larger offset gaps (yellow to orange) between the source and receiver lines in Figure 7 that is absent in Figure 6.

Figures 8 and 9 show expanded spider plots of a single CDP gather for each design. In these displays, the source-receiver pairs for every trace within the CDP gather are connected by a line segment. In Figure 9, the line spacings are constant and the relative position within the shot and receiver grid of each shot and receiver contributing to the CDP bin is exactly the same. Every trace in the CDP shown for the orthogonal design in Figure 9 comes from a shot in the second position below each receiver line and from the seventh receiver to the left of each shot line. In Figure 8, different source and receiver positions contribute within each CDP bin. This is caused by the variable line spacing, and induces the surface consistent statics coupling.

Figure 10 shows the resulting fold coverage for the recommended design over the survey area. It should be noted that the inner polygon (blue) inside the pink full-fold area represents the desired full-fold area. The outer (red) polygon represents the outline of the surface operations area bounding the source and receiver lines required to collect the full-fold data. A migration aperture has not been added to the full-fold area. The properly imaged area after migration will be smaller than the full-fold area by about 2000 m, which approximates the migration aperture for the deeper targets in this area.

Table 1 compares the cost function that was provided for the workshop as calculated for a number of different designs that were tested during this exercise. The baseline design parameters that result in a relative cost factor of 1.0 are shown first in the table for comparison purposes only. The second and third lines in the table represent the orthogonal and slant designs that were compared in detail above. Note that by using 1440 recording channels, rather than 720 as in the baseline case, 30-fold data in smaller CDP bins can be collected with improved economics. It should also be noted that the only difference between the orthogonal and slant designs is the distance between shot points along a shot line for surveying and move-up. Variable line spacing is completely cost neutral in operations.

The cost calculation is very sensitive to the number of geophones per receiver station. For this reason, testing should be done to determine the minimum acceptable geophone array. Acquisition experience in many areas has shown that 12 geophones per station is generally adequate, but if the number of geophones per group can be decreased to 6, the cost of the survey can be significantly reduced. In-line geophone and source arrays would be appropriate, though circular receiver arrays could be used for wide-azimuth acquisition.

Conclusions

I recommend 30-fold data in 20-mr square bins for this survey. The proposed recording template uses 10 active receiver lines each with 144 stations on 40-m group intervals, providing long offsets of about 3000 m in each bin. The nominal receiver and shot line intervals should be 400 and 480 m, respectively, providing adequate near offset coverage and wide azimuths, while minimising the shot point density. Variable line spacing should be used for receiver and shot lines to ensure surface consistent statics coupling. Slanted shot salvos will provide smoother offset distributions. 12 geophones per station should be adequate for recording the data, but arrays with just six geophones should be tested, potentially allowing significant cost savings. Finally, source parameters must also be tested at start-up.

Table 1: Cost Function Results for Various Tested Designs. The recommended design is highlighted on the third row of the table. This design should provide good geophysical results with neutral cost as compared to the baseline numbers provided, shown in the first row. If six geophones per receiver array can provide adequate signal-to-noise, then costs can be greatly reduced by minimising the receiver effort, as shown in the fourth row.

Active Cables	RCV Line Spacing	Geophones per Array	Group Interval	Active Channels	Shot Line Spacing	Shot Interval	Design Type	Nominal Fold	Cost Factor
6	400	24	50	720	400	50	Ortho	30	1
10	400	12	40	1440	480	40	Ortho	30	0.759
10	***400***	***12***	***40***	***1440***	***339.4***	***56.57***	***Slant***	***30***	***0.974***
10	***400***	***6***	***40***	***1440***	***339.4***	***56.57***	***Slant***	***30***	***0.649***
10	400	24	40	1440	339.4	56.57	Slant	30	1.623
12	400	12	50	1440	500	50	Ortho	36	0.678
12	400	12	40	1728	480	40	Ortho	36	0.892
10	400	12	50	1200	500	50	Ortho	30	0.599

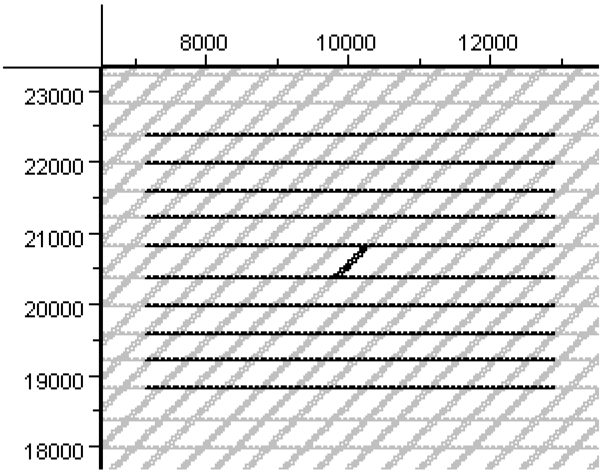

Figure 1. Recommended Slant Shooting Pattern

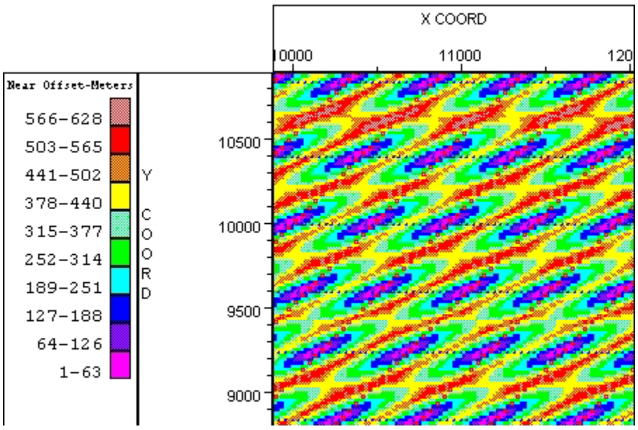

Figure 2. Near Offsets for the Recommended Slant Design

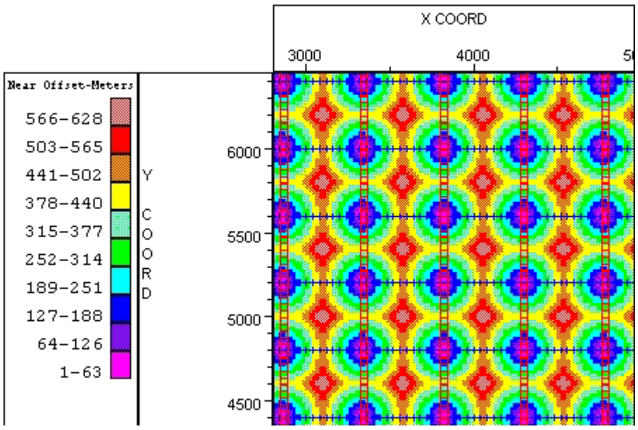

Figure 3. Near Offsets for a Comparable Orthogonal Design

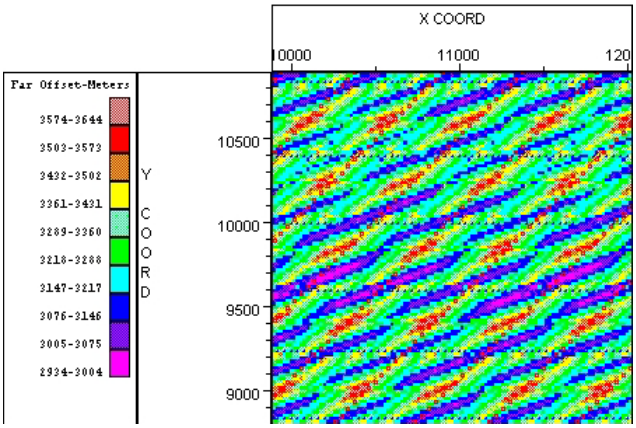

Figure 4. Far Offsets for the Recommended Slant Design

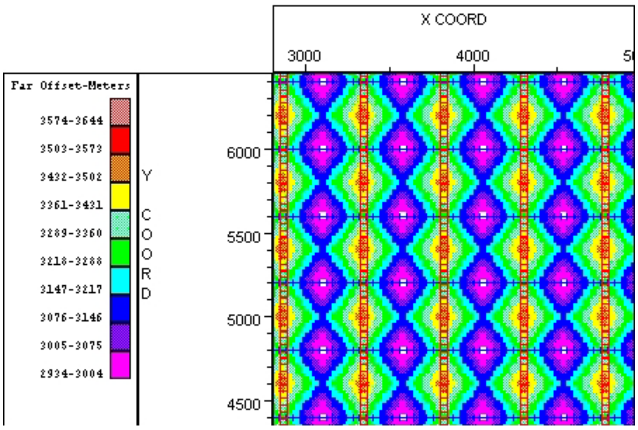

Figure 5. Far Offsets for a Comparable Orthogonal Design

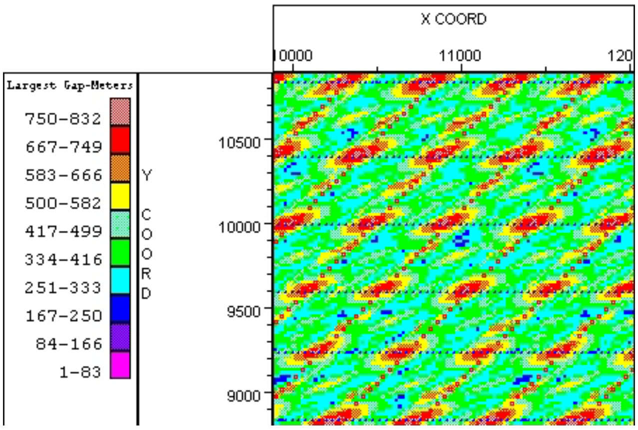

Figure 6. Maximum Offset Gaps for the Recommended Slant Design

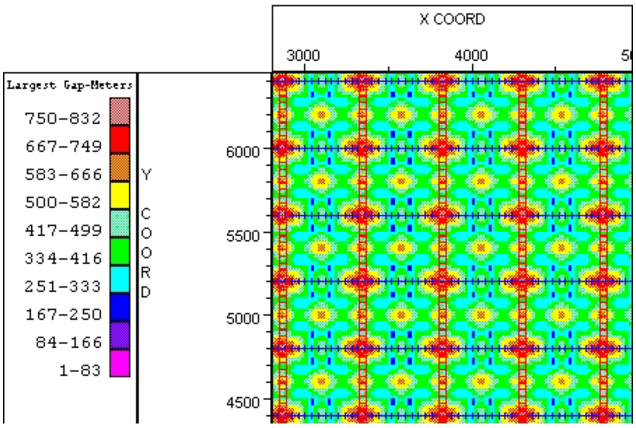

Figure 7. Maximum Offset Gaps for a Comparable Orthogonal Design

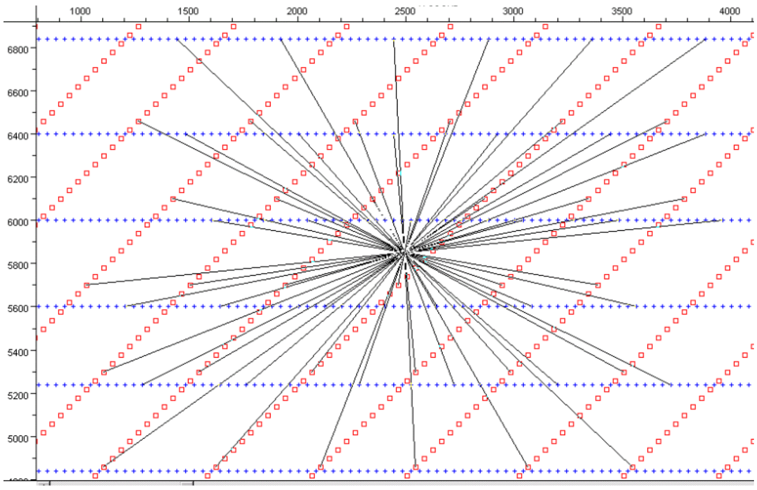

Figure 8. Expanded Spider Plot for the Recommended Slant Design

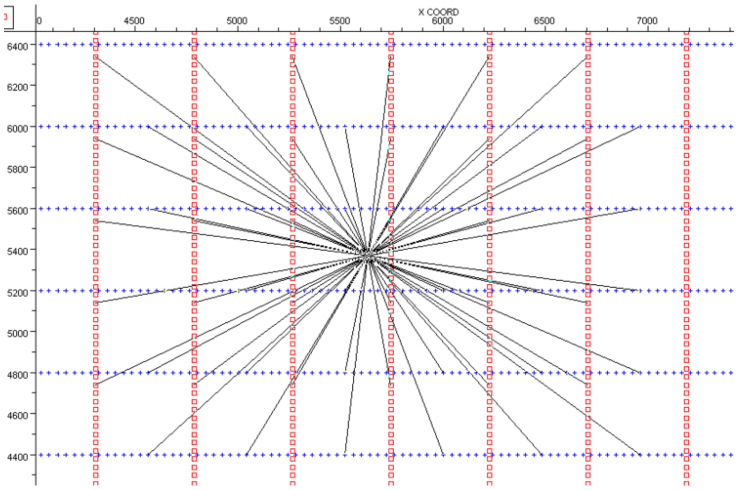

Figure 9. Expanded Spider Plot for a Comparable Orthogonal Design

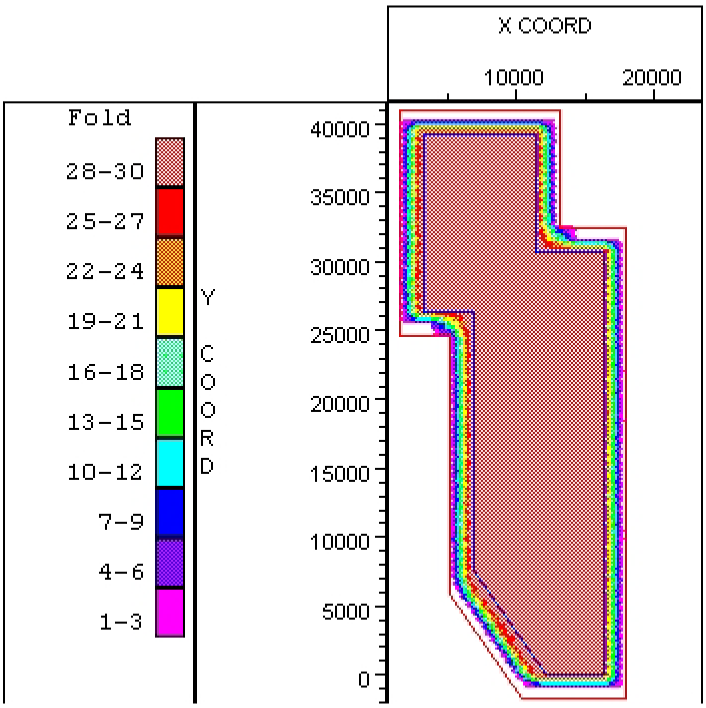

Figure 10. Fold Coverage Map for the Recommended Slant Design

Overview of solutions

Gijs J.O. Vermeer (3DSymSam - Geophysical Advice) and Kees Hornman (Shell Gabon)

In this concluding paper, we give a quick overview of the various solutions offered by the five specialists. The purpose of this review is not to present a verdict on their relative quality. The reader must make that judgement for himself.

Table 1 provides a comparison of all relevant parameters of the six solutions. This overview shows that a common set of information may be interpreted and translated into a survey design in widely different ways. Even after having heard each other's solutions, none of the designers changed his design; the designs presented here are the same as those presented at the Workshop.

In the first place, the choice of geometry varies: most designers select the orthogonal geometry, but Musser chose a slanted geometry (with varying source line and receiver line intervals!) and Galbraith opted for a double zigzag.

Fold, binsize and trace density are also widely different. This is illustrated in Figure 1. All designers chose a shot-point interval equal to the receiver station interval (strictly speaking, Musser and Galbraith chose a shot-point interval which was √2 times the receiver station interval). Apart from this, none of the designers followed 3D symmetric sampling theory (Vermeer, 1998).

During the design phase, there was hardly any interaction between the designer and the "client". This led to different assumptions between different designers. Most likely, this would have been quite different in real life. For instance, Lansley assumed that the prescribed resolution was a hard fact, whereas the other designers assumed that frequencies above 70 Hz would not be possible anyway. The client might have been able to say which one of the assumptions was valid, or that field tests would have to establish the maximum frequency.

Apart from comparing the final designs it is interesting to compare the reasonings used to arrive at the final recommendation. It is fair to say that all designers were limited by the space in which to describe their solution. This meant that none of them dealt in the same detail with all aspects to be covered in 3D survey design. There is quite a variety in emphasis and not too much overlap in the different papers.

Some aspects of 3D survey design are mentioned by only one of the five designers. A discussion of source design in relation to signal-to-noise ratio can be found in Meunier and Gillot's paper. Lansley discusses the effect of velocity errors on resolution; he also points out the effect of intra-array statics. Monk and Yates demonstrate the importance of curved raypaths for the choice of fringe area around the survey, and they mention the DMO effect on the size of the fringe. Musser has a special way of arriving at the maximum offset, and he ensures full statics coupling by recommending to use variable line spacings. Galbraith, when comparing potential survey designs, includes linear noise, multiple and DMO effects in his analyses.

Not all of these unique features lead necessarily to an improved choice of acquisition geometry, but it would be interesting to combine the best ideas and to design on basis of those. Or, if all designers would sit together for some time, would they be able to agree on a single compromise solution?

All in all, we learned a lot from this exercise. We trust the reader will enjoy comparing the various solutions as well.

Reference

Vermeer, G.J.O., 1999, 3-D symmetric sampling: Geophysics, **63**, 1629-1647.

Table 1 1999 EAGE 3D Seismic Design Workshop, comparision of submitted survey designs

Geometry parameters	**Meunier & Gillot I**	**Meunier & Gillot II**	**Lansley**	**Monk & Yates**	**Musser**	**Galbraith**
Overall geometry type	Orthogonal	Orthogonal	Orthogonal	Orthogonal	Slant	Double zig-zag
Bin size (m)	20 by 20	25 by 25	12.5 by 12.5	30 by 30	20 by 20	25 by 25
Inline fold x crossline fold	5 x 5	5 x 8	16 x 6	8 x 4	6 x 5	36 x 3
Live cable length (m)	5600	6000	8000	7680	5760	7200
Number of live cables	10	8	12	8	10	6
Max offset (m)	4134	5458	4660	4380	3529	3650
Max of min offsets (m)	684	686	472	722	628	about 200
Crossline roll	5	8	1 or 6	1	1	1
Source parameters						
Upper frequency goal (Hz)	65	65	110	60	90	70
Shot line interval (m)	560	600	250	480	variable, 480 +/- 40	100
SP interval (m)	40	50	25	60	40	50
Number of SP/salvo	55	128	16	9	avg 10	4
Number of SP/km^2	44.64	66.67	160	34.72	52.08	200
Receiver parameters						
Receiver line interval (m)	440	400	400	540	variable, 400 +/- 40	200
Receiver group interval (m)	40	50	25	60	40	50
Number groups/live cable	140	120	320	128	144	144
Number groups/km^2	56.82	50	100	30.86	62.5	100
Number of active channels	1400	960	3840	1024	1440	864
No. geophones/station	18	24	3 or 6	not stated	6 or 12 (test)	not stated
Distribution	3 rows of 6	2 lines of 12	1 row	not stated	1 row or circular	not stated

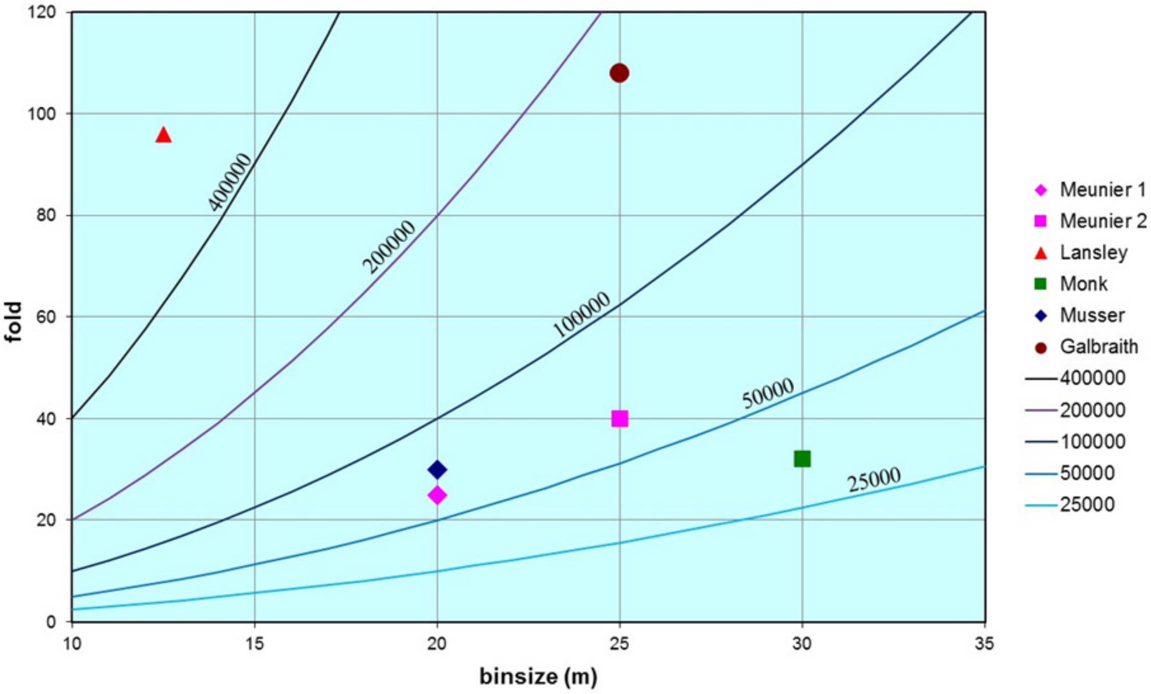

Figure 1 Fold versus binsize for six 3D survey designs. Curved lines indicate constant trace density in number of traces per km^2.